JOC*Article*

Enols of Substituted Cyanomalonamides

Ahmad Basheer,[†] Hiroshi Yamataka,[‡] Salai Cheettu Ammal,[‡] and Zvi Rappoport*,[†]

Department of Organic Chemistry, The Hebrew University, Jerusalem 91904, Israel, and Department of Chemistry, Rikkyo University, Nishi-Ikebukuro 3-34-1, Toshima-ku, Tokyo 171-8501, Japan

zr@vms.huji.ac.il

Received April 26, 2007

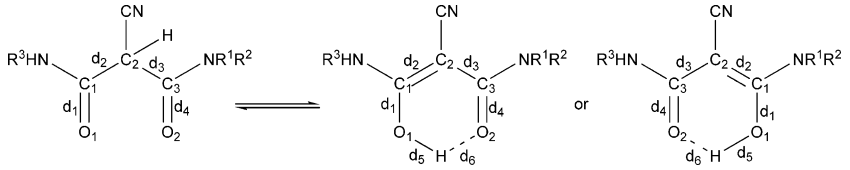

Twenty open-chain mono-, di-, and trialkyl and aryl-*N*-substituted cyanomalonamides $R^2R^1NCOCH(CN)CONHR^3$ were prepared. In solution, signals for both amide and a single enol are mostly observed, despite the potential for *E* and *Z* isomeric enols. The equilibrium (K_{Enol}) values between the amides and the enols were determined in different solvents by NMR spectra. They decrease on increasing the polarity of the solvent in the order $CDCl_3 \sim C_6D_6 > THF\text{-}d_8 > (CD_3)_2CO > CD_3CN > DMF\text{-}d_7 > DMSO\text{-}d_6$. For the $R^1R^2NCOCH(CN)CONHR^3$ system when $R^1 = R^2 =$ H, Me or $R^1 =$ H, $R^2 =$ Me, K_{Enol} for R^3 follows the order: $C_6F_5 >$ Ph $\geq$ An $\geq$ *i*-Pr $\geq$ *t*-Bu, and for R^1, R^2:H, H > Me, H > Me, Me in all solvents. A unique feature is the appreciable % enol in DMSO-d_6 when $R^1 = R^2 =$ H, in contrast with enol systems with other electron-withdrawing groups (EWGs). Calculations (B3LYP/6-31G**) corroborate the higher K_{Enol} values for less alkyl-substituted systems, showing that in the most stable conformer when $R^1 =$ H, $R^2 = R^3 =$ Me the *N*-hydrogens are closer to the CN group. The order of promoting substituents for enol of amide formation is $CONH_2 > CO_2CH_2CF_3 > CO_2Me >$ CONHMe. The solid-state structures of the isolated species, determined by X-ray crystallography, were either amides or enols, and a higher $K_{Enol}(CDCl_3)$ value does not ensure a solid enol structure. In no system were both solid species isolated. The X-ray structures of the enols were temperature-dependent. In most cases, the difference between the O−H and O···H bond lengths at low temperature were appreciable, but they become closer at the higher temperature. Similar tendency for either the C═C/C−C or the C−O/C═O bonds was observed. This is ascribed to a hydrogen shift between two regioisomeric enols in an asymmetric double-well potential, which becomes faster at a higher temperature. Calculations show that the enol structures are nonsymmetrical, resembling the lower temperature structures, even when they are chemically symmetrical, but the energy differences between the two regioisomers are <1 kcal. The hydrogen bonds in the enol moiety are strong, with O···O distances <2.45 Å, and are resonance-assisted hydrogen bonds. IR spectra in solution and the solid state qualitatively corroborate the NMR and X-ray structure determination.

Introduction

In our previous work on enols of carboxylic acid amides,[1] we had shown that long-lived enols of amides **1a** can be obtained if the amide **2a** ↔ **2b** carries two β-electron-withdrawing groups (EWGs) Y, Y′. This is mainly due to the contribution of the dipolar structure, in which the negative charge is delocalized as in **1b** over the two β-EWGs (eq 1 in Scheme 1). This enabled us to calculate the equilibrium constants for the enolization, K_{Enol} (or $pK_{Enol} = -\log K_{Enol}$), under various conditions.

From our data when Y, Y′ = CO_2R,[1a,c] CN,[1b] or SO_2R^2 groups, enolization is always on the amide carbonyl. In contrast,

[†] The Hebrew University.
[‡] Rikkyo University.

(1) (a) Mukhopadhyaya, J. K.; Sklenak, S.; Rappoport, Z. *J. Am. Chem. Soc*. **2000**, *122*, 1325. (b) Mukhopadhyaya, J. K.; Sklenak, S.; Rappoport, Z. *J. Org. Chem*. **2000**, *65*, 6856. (c) Lei, Y. X.; Cerioni, G.; Rappoport, Z. *J. Org. Chem*. **2001**, *66*, 8379. (d) Lei, Y. X.; Casarini, D.; Cerioni, G.; Rappoport, Z. *J. Org. Chem*. **2003**, *68*, 947. (e) Lei, Y. X.; Casarini, D.; Cerioni, G.; Rappoport, Z. *J. Phys. Org. Chem*. **2003**, *16*, 525. (f) Basheer, A.; Rappoport, Z. *J. Org. Chem*. **2004**, *69*, 1151.

10.1021/jo070877h CCC: $37.00
Published on Web 06/09/2007

SCHEME 1

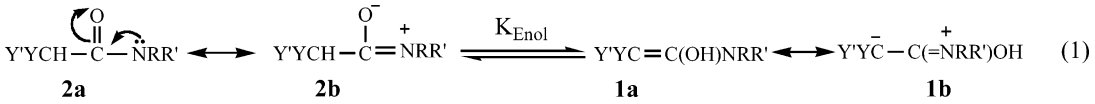

(1)

SCHEME 2

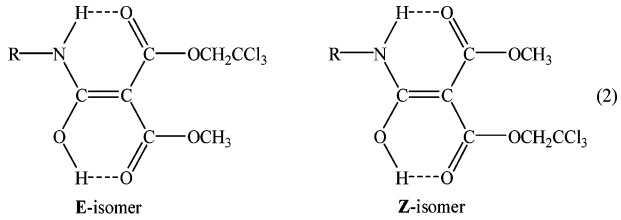

(2)

Stronger O···H-O H-bond
Weaker O···H-N H-bond

Weaker O···H-O H-bond
Stronger O···H-N H-bond

when enolization can take place on a Y or Y′ group rather than on the amide, both calculations[3] and experiment[1b] indicate that it will take place on them, for example, when Y is a C═O group of a ketone, except in special cases. Preferred enolization on a β-NO group was deduced from calculations.[4] With a NO_2 group, it is not easy from the experimental data obtained so far to distinguish between enolization on the amide or on the NO_2 group,[1b] although calculations[4] and experimental data for nitromalonamide[5] indicate enolization on the amide group.

Intramolecular hydrogen bonds play an important role in directing the enolization process, by contributing to increased enol stability.[1] This is shown by the lower field position of the OH in the more stable isomer of the *E/Z* enol pairs,[1c−f] as well as in the short O···O distances when one oxygen is of the enol and the other is of a β-ester group.[1c−f] This is demonstrated in eq 2 in Scheme 2, which shows an enol stabilized by an ester group where the *E* isomer is preferred since an O···H−O is stronger than an O···H−N H-bond.[6] In the solid state at low temperature, the hydrogen is located on the amide carbonyl rather than on the ester carbonyl.[1c] This is corroborated by calculations and by the appearance of two enols in solution when Y, Y′ are two different ester groups[1c−f] but of only one enol when the two ester groups are identical.[1c]

Several reasons exist to study a system with two amides as β-EWG groups (i.e., Y-substituted malonamides, YCH(CONR^{1}R^2)(CONR^{3}R^4)). A rare example of a known stable solid enol of amide is the formally symmetric nitromalonamide **3**[5] having an extremely short O(1)···O(2) nonbonding distance of 2.384 Å and a nonsymmetrical hydrogen bond.

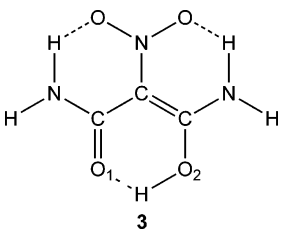

3

Its stability contrasts the small percent of enolization of system **1a/2a**, R = H, R′ = Ph, Y = NO_2, Y′ = CO_2Et.[1b] The effect of the four *N*-substituents R^1−R^4 appearing on both C_α and C_β, which have opposite electronic demands on enolization on the K_{Enol} values, is interesting. The enolization site is of interest if the two amide groups differ. However, if the hydrogen bond is either a single minimum or a double minimum with a rapid equilibration between two structures,[7] this question is meaningless. Finally, we want to compare the effect of an amido group with that of other EWGs as enolization promoting groups.

We have therefore prepared >20 Y-substituted malonamides and studied their enolization and the structures and properties of their enols under various conditions. Since a single activating group on an amide is insufficient to generate an observable enol, Y should be another EWG. In order to avoid a possible involvement of the group Y as an alternative enolization site or as a hydrogen-bonding partner (cf. the nitro group in **3**), we studied the cyanomalonamide systems **4**/**5**/**6** with Y = CN (eq 3 in Scheme 3). Previous experience showed that cyano is effective in promoting enol formation[1b,e] and that enolization on the cyano nitrogen to form a ketenimine does not compete with enolization on a geminal amide carbonyl. Moreover, the linear small cyano group is expected to reduce steric effects and not to be involved in intramolecular H-bonds with the enolic OH since the CN nitrogen and OH are too remote. Systems with other Y's will be discussed elsewhere.

Results and Discussion

Synthesis. The 20 cyanomalonamides were prepared by the reaction of the anion of substituted cyanoacetamide with aryl or alkyl isocyanates R^{3}NCO (eq 4 in Scheme 4). This gave the amides (**4**) or their enols (**5** or **6**) with at most three nitrogen substituents, that is, R^4 = H (eq 3).

NMR Data. ^{1}H and ^{13}C NMR spectroscopies were used to probe the structures of the enols/amides in solution and to calculate the K_{Enol} values. Both species were observed in the NMR spectra in most solvents. Although there are potentially both *E*- and *Z*-enols as well as regioisomeric enols (due to the two amido carbonyls), only signals for an apparent one enol species were observed. The enols were identified unequivocally by a very low-field ^{1}H δ(OH) signal at δ 16.16−19.02 which was observed for all of the enols investigated in most solvents (Table 1). The Table shows (a) that electron withdrawal shifts the OH to higher field, (b) that with two hydrogens on one nitrogen the OH is at a higher field, (c) that mostly in C_6D_6 the OH is at the highest field (e.g., for **5d**/**6d** δ(OH) = 19.02), and (d) that in some cases the OH is observed also in DMSO-d_6 and DMF-d_7 (e.g., in **5l-p**/**6l-p**). Generally, the δ(OH) values are at a lower field than for the enols of diester **1**, Y, Y′ = CO_2R, CO_2R′ or of a cyanoester **1**, Y = CN, Y′ = CO_2R.[1] The δ(NH) of the enol is at a lower field than that of the isomeric

(2) Basheer, A.; Rappoport, Z. Presented in the 9th European Symposium on Organic Reactivity (ESOR 9), Oslo, Norway, July 12−17, 2003; Abstr. OR 59, p 128, and the 17th IUPAC Conference on Physical Organic Chemistry, Shanghai, China, August 15−20, 2004; Abstr. IL-10, p 84.

(3) Sklenak, S.; Apeloig, Y.; Rappoport, Z. *J. Am. Chem. Soc.* **1998**, *120*, 10359.

(4) Yamataka, H.; Ammal, S. C. Unpublished results.

(5) Simonsen, O.; Thorup, N. *Acta Crystallogr., Sect. B* **1979**, *57*, 1177.

(6) Grabowski, S. J. *J. Phys. Org. Chem.* **2004**, *17*, 18.

(7) (a) Schuster, P.; Zundel, G.; Sandorfy C. In *The Hydrogen Bond. Recent Developments in Theory and Experiments*; North Holland: Amsterdam, 1976. (b) Hibbert, F.; Emsley, J. *Adv. Phys. Org. Chem.* **1990**, *26*, 255.

SCHEME 3

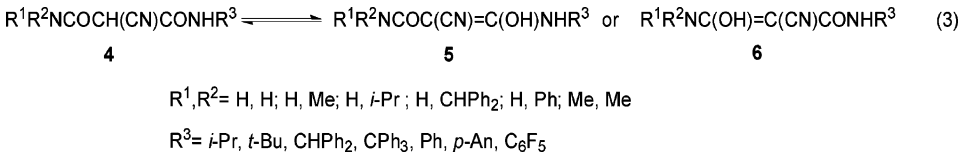

SCHEME 4

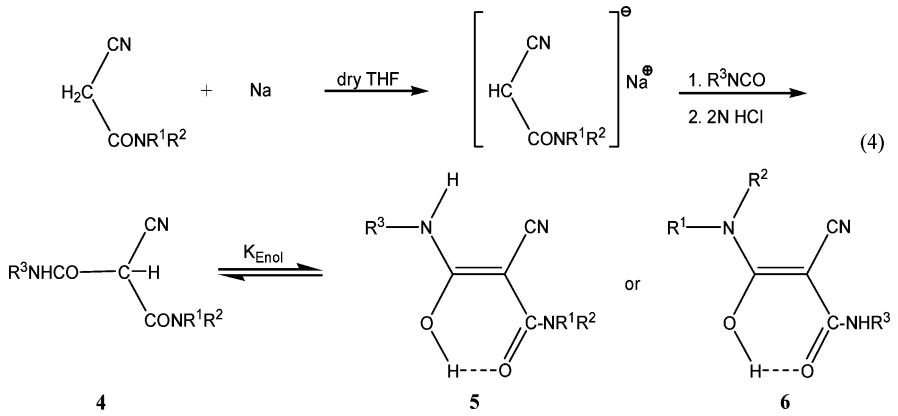

a: R^1= R^2= Me, R^3= Ph
b: R^1= R^2= Me, R^3= *p*-An
c: R^1= R^2= Me, R^3= C_6F_5
d: R^1= R^2= Me, R^3= *i*-Pr
e: R^1= R^2= Me, R^3= *t*-Bu
f: R^1= R^2= Me, R^3= CPh_3
g: R^1= H, R^2= Me, R^3= Ph
h: R^1= H, R^2= Me, R^3= *p*-An
i: R^1= H, R^2= Me, R^3= C_6F_5
j: R^1= H, R^2= Me, R^3= *i*-Pr
k: R^1= H, R^2= Me, R^3= *t*-Bu
l: R^1= R^2= H, R^3= Ph
m: R^1= R^2= H, R^3= *p*-An
n: R^1= R^2= H, R^3= C_6F_5
o: R^1= R^2= H, R^3= *i*-Pr
p: R^1= R^2= H, R^3= *t*-Bu
q: R^1= H, R^2= Ph, R^3= C_6F_5
r: R^1= H, R^2= Ph, R^3= Ph
s: R^1= H, R^2= *i*-Pr, R^3= *i*-Pr
t:: R^1= H, R^2= $CHPh_2$, R^3= $CHPh_2$

amide, and the δ(NH)[amide] − δ(NH)[enol] difference is higher in the nonpolar solvents.

The spectra also show the two enol NH signals, as well as the CH and the two NH signals of the amide. The NH signals were identified by their relative integrations compared with the OH and CH signals. An example of the spectrum of the **4e**/**5e**/**6e** system displaying both the *Z*-enol (see below) and the amide (Figure 1) is simple despite the potential problems mentioned above. Separate signals for the amide and enol are observed, so that they do not equilibrate rapidly on the NMR time scale of the experiment. Unidentified signals are observed for the polyaryl-substituted **4f**/**5f**/**6f** and **4t**/**5t**/**6t** and are ascribed to decomposition; **4k**/**5k**/**6k** display signals which may be due to their derived anion formed in THF-d_8 (18%), CD_3CN (39%), and DMF-d_7 (100%).

The enol/amide ratios were calculated from the integrations of pairs of signals, such as OH versus CH, the Ph−H, $MeOC_6H_4$, or NH signals for the aryl-substituted systems, and *i*-Pr or *t*-Bu signals of both species for the *N*-alkyl-substituted systems. The differences between the percentages determined for a species by different methods were mostly 2−4%. The average values were used to obtain the K_{Enol} values given in Table 1. The relative integrations of all signals are given in Table S1 in the Supporting Information.

The ^{13}C NMR spectral data (Table S3 in the Supporting Information) are in line with the ^1H NMR data (Tables 1 and S1) and provide a qualitative characterization for the amides and their enols. Two pairs of low-field signals were observed. The lower pair for the enol appears at 170.62−173.18 and 171.17−175.16 ppm and is ascribed to C═O and C_α, respectively, compared with the two amide C═O groups at 157.58−162.97 ppm. The amide CN signals appear in the C/H coupled spectra as doublets (J = 10.6−11.3 Hz) at a higher field (113.04−116.12 ppm) than the enol CN singlets at 115.01−121.08 ppm. Finally, the coupled C_β doublets (J = 136.4−138.9 Hz) of the amides appear at 42.46−48.92 ppm, a lower chemical shift than that of the enol C_β singlets at 53.51−57.88 ppm.

Substituent and Solvent Effects on K_{Enol} Values. Table 1 displays K_{Enol} values for 19 cyanomalonamides in 5−7 solvents and for the **4f**/**5f**/**6f** system in 3 solvents. As with all the other activated enols of amides previously studied,[1] increase in the dielectric constant of the solvent results in a lower % enol. This is ascribed to the higher polarity of the amides than of the internally hydrogen bonded, that is, internally solvated, and hence of lower polarity enols, which consequently require less external solvation.[1c] A similar explanation was suggested for the solvent effect on K_{Enol} of 1,3-dicarbonyl compounds whose enols can form intramolecular hydrogen bonds.[8] In contrast, simple enols of ketones, aldehydes, or 1,3-diketones incapable of forming strong hydrogen bonds display higher % enol in the more polar and hydrogen-bonding solvents.[9]

However, a remarkable feature of the enols of cyano- (and nitro-)[10] malonamides is that several of them, especially when singly *N*-substituted (Table 1 and see below), are observable in

(8) Floris, B. In *The Chemistry of Enols*; Rappoport, Z., Ed.; Wiley: Chichester, 1990; Chapter 4, p 147.

(9) (a) Miller, A. R. *J. Org. Chem.* **1976**, *41*, 3599. (b) Koelle, U.; Forsen, S. *Acta Chem. Scand. Ser. A* **1974**, *28*, 531. (c) Rochlin, E.; Rappoport, Z. *J. Am. Chem. Soc.* **1992**, *114*, 230.

(10) The chemistry of nitromalonamide and derivatives will be discussed elsewhere.

TABLE 1. δ(OH), δ(CH), and δ(NH) Spectral Data and R^1, R^2, and R^3 Effect on K_{Enol} for the $R^3NHCOCH(CN)CONR^1R^2$/ $R^3NHC(OH)=C(CN)CONR^1R^2$/$R^3NHCOC(CN)=C(OH)NR^1R^2$ (4/5/6) System in Several Solvents at Room Temperature

		Enol			Amide					
compound	solvent	δ(OH)	δ(NH)1	δ(NH)2	δ(CH)	δ(NH)1	δ(NH)2	% enol	K_{Enol}	pK_{Enol}
4a/5a/6a	$CDCl_3$	17.79	7.67		4.80	9.16		80	4.0	-0.60
	C_6D_6	18.41	7.96		4.32	9.49		80	4.0	-0.60
	THF-d_8	18.18	8.52		5.05	9.64		46	0.85	0.07
	$(CD_3)_2CO$	18.07	8.50		5.31	9.66		18	0.22	0.66
	CD_3CN	17.88	7.91		5.00	8.94		13	0.15	0.83
	DMF-d_7				5.57	10.62		0	$\leq$0.02	$\geq$1.7
	DMSO-d_6				5.43	10.45		0	$\leq$0.02	$\geq$1.7
4b/5b/6b	$CDCl_3$	17.88	7.66		4.75	9.14		80	4.0	-0.60
	C_6D_6	18.61	7.97		4.43	9.43		78	3.55	-0.55
	THF-d_8	18.19	8.51		5.06	9.56		44	0.79	0.10
	CD_3CN	18.02	7.86		5.00	8.73		13	0.15	0.83
	DMF-d_7		8.45		5.51	10.48		5	0.052	1.28
	DMSO-d_6				5.39	10.34		0	$\leq$0.02	$\geq$1.7
4c/5c/6c	$CDCl_3$	16.82	7.44		4.84	9.40		93	13.3	-1.12
	C_6D_6	17.46	7.65		4.10	9.37		95	19.0	-1.28
	THF-d_8	17.46	8.81		5.26	9.85		77	3.35	-0.52
	CD_3CN	16.95	7.76		5.15	8.76		39	0.64	0.19
	DMF-d_7	17.39	9.81		5.83	10.89		15	0.18	0.75
	DMSO-d_6	17.28	9.91		5.69	10.73		7	0.08	1.12
4d/5d/6d	$CDCl_3$	18.18	5.62		4.61	6.68		80	4.0	-0.60
	C_6D_6	19.02	5.89		4.28	6.92		83	4.88	-0.69
	THF-d_8	18.53	6.37		4.80	7.31		63	1.70	-0.23
	$(CD_3)_2CO$	18.51	6.47		5.03	7.47		28	0.39	0.41
	CD_3CN	18.36	6.00		4.80	6.85		13	0.35	0.45
	DMF-d_7	18.59	7.40		5.23	8.35		7	0.08	1.12
	DMSO-d_6	18.42	5.49		5.12	8.36		4	0.04	1.38
4e/5e/6e	$CDCl_3$	18.24	5.66		4.51	6.59		73	2.70	-0.43
	C_6D_6	18.91	5.85		4.01	6.87		80	4.0	-0.60
	THF-d_8	18.37	5.98		4.70	7.19		47	0.89	0.05
	$(CD_3)_2CO$							28	0.39	0.41
	CD_3CN	18.30	5.80		4.72	6.70		8	0.09	1.06
	DMF-d_7	18.40	6.55		5.20	8.22		2	0.02	1.66
	DMSO-d_6				5.07	8.15		0	$\leq$0.02	$\geq$1.7
4f/5f/6f	$CDCl_3$	17.52	7.10		4.54	8.17		74	2.85	-0.45
	CD_3CN	17.39	6.33		4.96	8.17		8	0.09	1.06
	DMSO-d_6				5.49	9.37		0	$\leq$0.02	$\geq$1.7
4g/5g/6g	$CDCl_3$	17.65	7.40	6.04	4.63	9.21	*f*	90	9.0	-0.95
	C_6D_6	18.34	7.40	5.32	3.78	9.18	6.12	92	11.5	-1.06
	THF-d_8	18.18	8.58	7.32	4.60	9.68	7.77	84	5.25	-0.72
	CD_3CN	17.89	7.87	6.51	4.65	8.95	7.00	52	1.08	-0.03
	DMF-d_7	18.21	9.59	8.05	5.08	10.53	8.38	30	0.43	0.37
	DMSO-d_6	18.16	9.61	*f*	4.90	10.38	8.33	18	0.22	0.66
4h/5h/6h	$CDCl_3$	17.71	7.16	5.76	4.56	8.96	7.23	90	9.0	-0.95
	C_6D_6	18.47	7.08	5.00	5.60	7.36	5.85	90	9.0	-0.95
	CD_2Cl_2	17.70	7.09	5.68	4.49	8.85	*f*	85	5.67	-0.75
	THF-d_8	18.25	8.53	7.23	4.54	9.56	7.76	84	5.25	-0.72
	CD_3CN	17.96	7.76	6.42	4.59	8.77	7.08	57	1.33	-0.12
	DMF-d_7	18.31	9.56	7.46	5.04	10.42	8.38	31	0.45	0.35
	DMSO-d_6	*a*	9.52	7.97	4.85	10.24	8.29	16	0.19	0.72
4i/5i/6i	$CDCl_3$	16.70	7.16	6.06	4.69	9.25	6.94	97	32.3	-1.51
	C_6D_6	17.29	6.73	4.92	3.39	8.88	5.55	97	32.3	-1.51
	THF-d_8	17.35	8.89	7.61	4.78	9.84	7.82	96	24	-1.38
	CD_3CN	16.91	7.70	6.68	4.79	8.87	7.02	79	3.76	-0.58
	DMF-d_7	17.03	9.87	8.25	5.29	10.77	8.25	69	2.23	0.35
	DMSO-d_6	17.09	9.81	8.42	5.07	10.60	8.42	56	1.27	-0.11
4j/5j/6j	$CDCl_3$	17.73	5.37	5.74	4.39	6.88	7.14	92	11.5	-1.06
	C_6D_6	18.70	5.45	5.45			*f*	100	$\geq$50	≤ -1.7
	THF-d_8	18.44	6.56	6.91	4.26	7.49	7.59	90	9.0	-0.95
	CD_3CN	18.11	5.99	6.24	4.38	6.88	6.95	54	1.17	-0.07
	DMF-d_7	18.39	7.58	7.67	4.77	8.32	8.32	46	0.85	0.07
	DMSO-d_6	18.26	7.57	7.67	4.59	8.13	8.15	25	0.33	0.48
4k/5k/6k	$CDCl_3$	17.80	5.31	5.58	4.32	6.81	7.01	84	5.25	-0.72
	C_6D_6	18.65	5.04	5.30	3.62	6.09	6.75	93	13.3	-1.12
	THF-d_8[a]	18.27	5.91	7.01	4.30	7.51	7.81	63	3.32	-0.52
	CD_3CN[b]	18.10	5.60	6.22	4.33	6.79	7.45	20	0.49	0.31
	DMF-d_7[c]	10.82[d]	7.40	8.35	10.82[d]	7.40	8.35	0	$\leq$0.02	$\geq$1.7
	DMSO-d_6	18.15	6.65	*f*	4.59	7.91	8.09	17	0.21	0.69

TABLE 1. Continued

		Enol			Amide					
compound	solvent	δ(OH)	δ(NH)1	δ(NH)2	δ(CH)	δ(NH)1	δ(NH)2	% enol	K_{Enol}	pK_{Enol}
4l/5l/6l	$CDCl_3$	17.32	7.30	5.48				100	≥50	≤−1.7
	C_6D_6	17.70	7.36	4.01				100	≥ 50	≤−1.7
	THF-d_8	17.35	8.53	4.72	4.58	9.66	7.39	97	32.3	-1.51
	CD_3CN	17.29	7.88	6.36	4.64	8.85	6.71	83	4.88	-0.69
	DMF-d_7	17.40	9.56	8.28	5.07	10.54	8.28	69	2.23	-0.35
	DMSO-d_6	17.00	9.53	7.90	4.68	10.36	7.37	43	0.75	0.12
4m/5m/6m	THF-d_8	17.54	4.84	7.23	4.73	10.84	*f*	94	15.97	-1.19
	$(CD_3)_2CO$	17.54	8.52	7.23	4.82	9.55	*f*	91	10.11	-1.0
	CD_3CN	17.43	7.81	6.29	4.61	8.73	7.06	81	4.26	-0.63
	DMF-d_7	17.56	9.44	8.20	5.03	10.53	*f*	74	2.85	-0.45
	DMSO-d_6	17.35	9.38	8.20	4.84	10.24	7.72	45	0.82	0.087
4n/5n/6n	$CDCl_3$	16.23	7.00	5.68				100	≥50	≤-1.7
	C_6D_6	16.57	6.51	4.09				100	≥50	≤-1.7
	THF-d_8	16.42	8.88	7.50				100	≥50	≤-1.7
	CD_3CN	16.16	7.79	6.59	4.83	8.83	6.81	95	13	-1.28
	DMF-d_7	16.29	9.82	8.31	5.03	10.78	8.99	92	11.2	-1.06
	DMSO-d_6	15.63	9.74	8.24	5.06	10.60	8.99	88	7.33	-0.87
4o/5o/6o	$CDCl_3$	17.53	5.36	5.36				100	≥50	≤-1.7
	C_6D_6	18.32	5.10	4.18				100	≥50	≤-1.7
	THF-d_8	17.89	6.55	6.93				100	≥50	≤-1.7
	CD_3CN	17.80	5.90	6.08	4.38	6.67	6.80	84	5.25	-0.72
	DMF-d_7	18.00	7.79	7.48	4.80	8.19	*f*	78	3.55	-0.55
	DMSO-d_6	17.76	8.13	*f*	4.59	7.60	3.36	40	0.67	0.18
4p/5p/6p	$CDCl_3$	17.59	5.43	5.43				100	≥50	≤-1.7
	C_6D_6	18.25	5.26	4.17				100	≥50	≤-1.7
	THF-d_8	17.61	5.87	6.96	4.78	7.30	7.35	94	15.7	-1.2
	CD_3CN	17.71	5.68	6.12	4.37	6.27	6.67	66	1.94	-0.29
	DMF-d_7	17.96	6.52	7.87	4.78	7.77	7.68	53	1.13	-0.05
	DMSO-d_6	17.53	6.51	7.68	4.58	7.89	7.56	33	0.49	0.31
4q/5q/6q	$CDCl_3$	17.27	7.04	7.28				100	≥50	≤-1.7
	C_6D_6	17.75	7.29	7.08				100	≥50	≤-1.7
	THF-d_8	17.76	9.18	9.26	4.89	9.90	9.75	87	6.69	-0.83
	CD_3CN	17.41	7.93	8.28	4.97	8.88	8.70	54	1.17	-0.07
	DMF-d_7				5.61	11.12	10.96	0	≤0.02	≥1.7
	DMSO-d_6				5.30	10.75	10.60	0	≤0.02	≥1.7
4r/5r/6r	$CDCl_3$	17.94	7.29	*e*	*f*	8.72	*e*	94	15.67	-1.19
	C_6D_6	18.41	6.91	*e*	5.51	8.26	*e*	93	13.29	-1.12
	THF-d_8	18.33	8.91	*e*	4.72	9.66	*e*	69	2.23	-0.35
	CD_3CN	18.06	8.07	*e*	4.83	8.72	*e*			
	DMF-d_7			*e*	5.29	8.00	*e*	0	≤0.02	≥1.7
	DMSO-d_6			*e*	5.12	10.40	*e*	0	≤0.02	≥1.7
4s/5s/6s	$CDCl_3$	17.76	5.38	*e*	4.41	6.88	*e*	89	8.09	-0.91
	C_6D_6	18.77	5.42	*e*	*f*	6.71	*e*	94	15.67	-1.1
	THF-d_8	18.38	6.60	*e*	4.27	7.50	*e*	85	5.67	-0.75
	CD_3CN	18.18	6.00	*e*	4.36	6.85	*e*	44	0.79	0.10
	DMF-d_7	18.43	7.50	*e*	4.71	8.09	*e*	38	0.61	0.21
	DMSO-d_6	18.29	7.51	*e*	4.54	8.04	*e*	19	0.23	0.36
4t/5t/6t	$CDCl_3$	17.69	6.03	*e*			*e*	100	≥50	≤-1.7
	C_6D_6	18.62	6.54	*e*			*e*	100	≥50	≤-1.7
	THF-d_8	18.39	7.70	*e*	4.78	8.78	*e*	62	1.63	-0.21
	CD_3CN	17.96	6.79	*e*	4.84	8.00	*e*	13	0.15	0.83
	DMF-d_7			*e*	5.50	9.50	*e*	0	≤0.02	≥1.7
	DMSO-d_6			*e*	5.18	9.29	*e*	0	≤0.02	≥1.7

[a] Ionization of 18%. [b] Ionization of 39%. [c] Ionization of 100%. [d] Signal ascribed to H^+. [e] $NHR^3 = NR^1R^2$. [f] Not observed.

significant percentage even in DMSO-d_6 and DMF-d_7. Previous studies with other amide/enol systems in these solvents either showed no enol or ionization to the enolate ion when substituted with strong EWGs.[1c−e] Likewise, contrary to the very low % enol previously observed in CD_3CN,[1c−e] the cyanomalonamides display 8−95% enol in CD_3CN.

The dependence of K_{Enol} on R^1, R^2 in all solvents is regular and appreciable. The % enol increases when the number of Me (and other alkyls) groups decreases and follows the order: R^1, R^2 = H, H > Me, H > Me, Me (Table 1, **a**−**p**). The cyanomalonamides are not soluble enough for determining K_{Enol} values in CCl_4. However, K_{Enol} values in $CDCl_3$ show systematic substituent effects (Table 1). For the NR^1R^2 derivatives, the % enol changes from 73 to 80% (K_{Enol} = 2.2−4.0) for the NMe_2 derivative to 84−92% (K_{Enol} = 5.3−11.5) for the NHMe derivatives and reaches 100% (K_{Enol} ≥ 50) for the NH_2 derivatives. Within the first group, the % enol is nearly the same for R^3 = *i*-Pr, *p*-An, and Ph and somewhat lower for R^3 = *t*-Bu and CPh_3. The highest % enol is for $R^3 = C_6F_5$.

For R^3 = *t*-Bu in $CDCl_3$, C_6D_6, and $(CD_3)_2CO$, and less in THF-d_8, the % enol resembles the values for R^3 = *i*-Pr, whereas the values in DMSO-d_6 are somewhat lower. With R^3 = Ph, the values in the less polar solvents resemble those for R^3 = *t*-Bu. In DMF-d_7 and DMSO-d_6, the enol was not observed for $R^1R^2 = Me_2$, but its percentage was significant, being 69 and 43 for $R^1R^2 = H_2$.

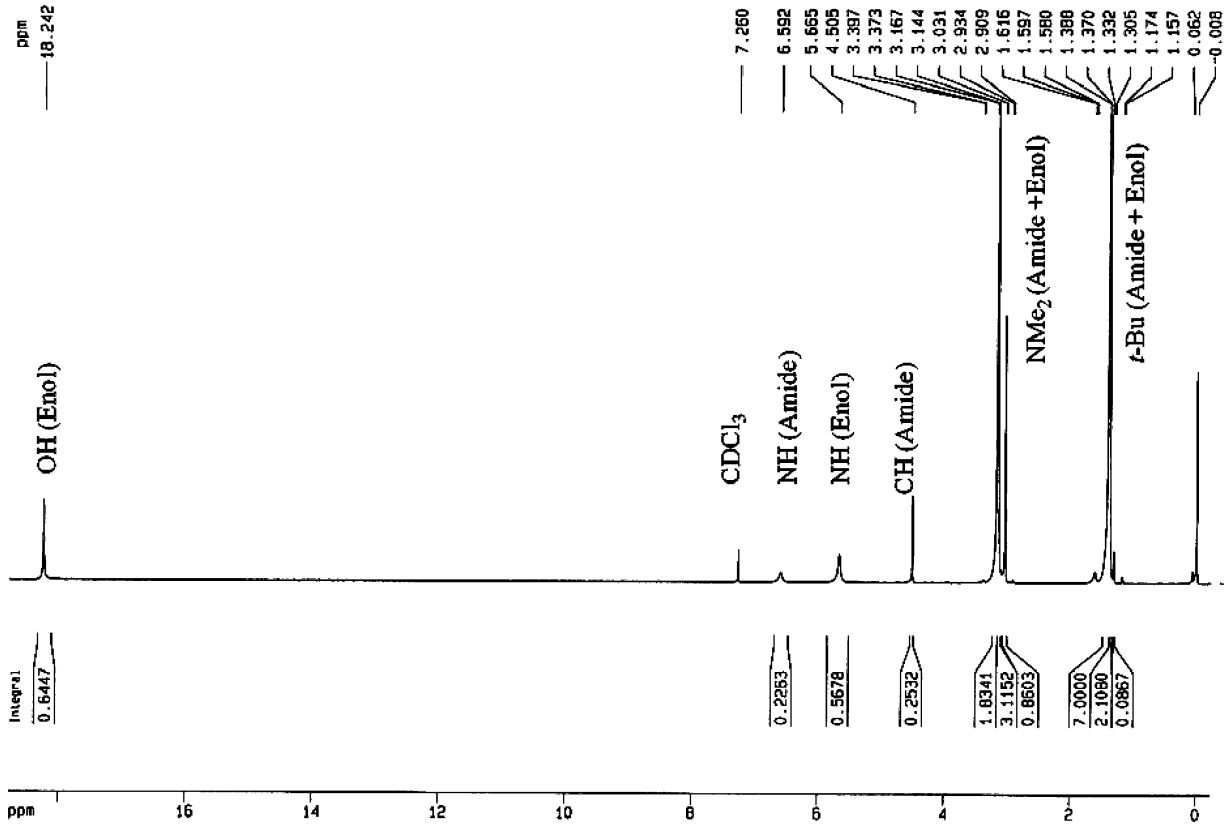

FIGURE 1. ^{1}H NMR spectrum of **4e**/**5e**/**6e** in $CDCl_3$.

In THF-d_8, a hydrogen-bonding solvent of a moderate polarity, the % enol is lower than that in $CDCl_3$, but the same trend for R^1R^2 is obtained, that is, 44−77% enol (K_{Enol} = 0.79−3.35) for NMe_2, 76−90% enol (K_{Enol} = 3.2−9.0) for NHMe, and 94−100% enol (K_{Enol} = 15.7 to ≥50) for NH_2. The highest % enol is for *i*-Pr for NH_2 and NHMe, and the second highest is for NMe_2. In the high dielectric constant DMSO-d_6, all the R^3, NMe_2 systems give no enol, similarly to almost all systems studied previously,[1] although with R^3 = *i*-Pr or C_6F_5, signals interpreted as those of 4 and 7% enol were observed. However, for the R^3, NHMe systems, the % enol is already 16−25% (K_{Enol} = 0.19−0.33), except for $R^3 = C_6F_5$, which displays 56% enol (K_{Enol} = 1.27). For the R^3, NH_2 system, the % enol is 33−45% (K_{Enol} = 0.49−0.82), except when $R^3 = C_6F_5$ (88% enol, K_{Enol} = 7.33, Table 1). In CD_3CN, there is 8−13% enol for the NMe_2 (39% for $R^3 = C_6F_5$), 20−57% enol for the NHMe (79% for $R^3 = C_6F_5$), and 66−84% enol for the NH_2 (95% for $R^3 = C_6F_5$).

C_6D_6 gave very similar % enol to $CDCl_3$ for several R^3, NMe_2 systems, except when R^3 = *t*-Bu (higher % in $CDCl_3$). The difference, in the same direction, is higher for the R^3 = *i*-Pr, *t*-Bu, NHMe systems. For the NH_2 systems, the % enol is 100% for all derivatives (Table 1). Interestingly, DMF-d_7 consistently displays higher % enol (53−78%, $R^1R^2 = H_2$) than DMSO-d_6 (33−45%, $R^1R^2 = H_2$) and lower % than CD_3CN (66−95%, $R^1R^2 = H_2$). The % enol in $(CD_3)_2CO$ for selected systems shows that it is between THF-d_8 and CD_3CN (Table 1).

The % enol is higher for $R^3 = C_6F_5$ than for R^3 = Ph, *p*-An (aromatic substituents) and for R^3 = *i*-Pr than for R^3 = *t*-Bu or CPh_3 (aliphatic substituents). The effect of R^3 on % enol is relatively small, and when $R^1 = R^2$ = H, Me or R^1 = H, R^2 = Me, it follows the order: C_6F_5 > Ph ≥ An ≥ *i*-Pr ≥ *t*-Bu. In summary, the solvent effect is similar to that found earlier with other amide/enol systems[1] where increase in the dielectric constant of the solvent results in a decreased K_{Enol} value which follows the order: $CDCl_3 \sim C_6D_6$ > THF-d_8 > $(CD_3)_2CO$ > CD_3CN > DMF-d_7 > DMSO-d_6.

Three symmetrical systems where the substituents R^1,R^2 = R^3,R^4 are H, Ph (**4r**/**5r**/**6r**), H, *i*-Pr (**4s**/**5s**/**6s**), or H, $CHPh_2$ (**4t**/**5t**/**6t**) were investigated (Table 1). Symmetry does not increase the enol stability compared with the slightly less symmetric systems with R^1,R^2 = HPh, R^3,R^4 = NHMe or R^1,R^2 = NHPh, R^3,R^4 = NHC_6F_5 and R^1,R^2 = NHPr-*i*, R^3,R^4 = NHMe substituted pairs. In most cases, the less symmetrical system gives higher K_{Enol} (e.g., K_{Enol} = 2.23 when R^1,R^2 = R^3,R^4 = HPh compared with K_{Enol} = 6.69 when R^1,R^2 = R^3,R^4 = HPh, HC_6F_5 or K_{Enol} = 5.25 when R^1,R^2 = R^3,R^4 = HPh, HMe in THF-d_8) regardless if the steric effect is increased or decreased. The "exceptions" are cases where K_{Enol} is very high (>90%) and its error is therefore large. K_{Enol} value for the NHMe, NHPr-*i* (11.5 in $CDCl_3$) derivative is slightly higher than that for the NHMe, NHBu-*t* (5.52 in $CDCl_3$) one in all solvents, and we ascribe it to a small steric effect (Table 1). Similar effect was observed with the NMe_2, NHPr-*i* (4.0 in $CDCl_3$) and NMe_2, NHBu-*t* (2.7 in $CDCl_3$) pairs. However, for the $NHCHPh_2$, $NHCHPh_2$ system, the K_{Enol} value is ≥50 in $CDCl_3$ and C_6D_6, a higher value than for the NHPr-*i*, NHPr-*i* (**4s/5s/6s**) (8.09 in C_6D_6) system, but the value of 0% enol in DMF-d_7 and DMSO-d_6 was lower than the values of 38 and 19% enol for the latter system. A high steric effect is expected for the **4f/5f/6f** system, where R^1,R^2 = Me_2, R^3 = CPh_3. However, the K_{Enol} values of 2.85 in $CDCl_3$ and 0.09 in CD_3CN do not show an extreme steric effect. For an explanation see below.

Calculated pK_{Enol} Values. Calculated pK_{Enol} values were found in the past to be somewhat sensitive to the basis set

TABLE 2. Calculated (B3LYP/6-31G) pK_{Enol} Values at 298.15 K and Bond Lengths (in Å) of Enols Derived from $R^1R^2NCOCH(Y)CONR^3R^4$ at 0 K**

Y	R^1	R^2	R^3	R^4	O−H	O···H	O···O	pK_{Enol}
CN	H	H	H	H	1.050	1.454	2.445	-5.7
CN	H	Me	H	Me	1.054	1.437	2.437	-4.3
CN	Me	Me	Me	Me	1.067	1.383	2.400	-2.1
CN	H	H	H	*i*-Pr	1.050	1.452	2.443	-5.1
CN	H	*i*-Pr	H	*i*-Pr	1.055	1.436	2.437	-4.3
CN	H	Me	H	*i*-Pr	1.051	1.444	2.440	-4.2
CN	Me	Me	H	*i*-Pr	1.060	1.400	2.411	-4.1
CN	Ph	H	Me	Me	1.048	1.428	2.423	-4.7
CN	An	H	Me	H	1.065	1.409	2.423	-4.19
CN	C_6F_5	H	Me	H	1.038	1.485	2.461	-4.21
CN	C_6F_5	H	H	H	1.033	1.505	2.471	-5.19
H	H	H	H	H	1.035	1.504	2.474	5.8
NO_2	H	H	H	H	1.086[a]	1.344[a]	2.380[a]	-8.5

[a] Obs. O−H 1.01, O···H 1.44, O−H···O 2.384 Å (rt); 1.11, 1.28, 2.3730 Å (100 K).

used.[3,11] The calculations in this work are at the B3LYP/6-31G** level, in order to facilitate comparisons with previous calculations.[1a,3,11]

The calculated values for R^1-R^4 for 13 systems of special interest are given in Table 2. For the symmetrical system with R^1, $R^2 = R^3$, R^4, the pK_{Enol} value decreases with the increased methyl substitution on the two amido groups, being −5.7 for the parent cyanomalonamide, −4.3 for its *N*,*N*′-dimethyl derivative, and −2.1 for the *N*,*N*,*N*′,*N*′-tetramethyl derivative. When one amide derivative is fixed as a CONHPr-*i* and the other one is changed from $CONH_2$ to CONHMe to $CONMe_2$, the same trend is observed, but the values become much closer: pK_{Enol} = −5.1, −4.2, and −4.1, respectively. The trend is identical with that found experimentally, indicating that it is not due mainly to solvation, although the observed values are more negative. The similarity of the calculated K_{Enol} values for the **5d/6d** and **5j/6j** systems is due to the fact that the hydrogen of the NHPr-*i* moiety is located near the CN in both systems.

These systems display systematic changes in the O−H, O···H, and O···O distances (Table 2). The O−H bond elongates from 1.050 (R^1-R^4 = H), via 1.054 (R^1, R^3 = H, R^2, R^4 = Me) to 1.067 (R^1-R^4 = Me), and the O···H bond shortens, respectively, from 1.454, via 1.437 to 1.383 Å. The O···O distance decreases from 2.445 for the 4H to 2.400 Å for the 4Me compound. Again, the symmetrical NHPr-*i* derivative behaves similarly to the NHMe derivative. Table 2 also presents the calculated data for the enols of $YCH(CONH_2)_2$ for Y = H, NO_2. Compared with Y = CN, R^1-R^4 =H, O−H is shorter and O···H is longer for Y = H, and O−H is longer and O···H is shorter for Y = NO_2. The symmetry of the hydrogen bond, reflected by the calculated $\Delta_{OH} = d(O\cdots H)-d(O-H)$, is the lowest for the most stable enol with pK_{Enol} of −8.5 when Y = NO_2 (0.258 Å) and the highest for the least stable enol with Y = H (pK_{Enol} =5.8, Δ_{OH} = 0.469 Å). The values for the di- and tetra-Me systems follow this trend, the more negative the pK_{Enol} value, the lower the Δ_{OH} value.

The energies of the four stable conformers of the enol with R^1, $R^2 = R^3$, R^4 = Me, H were calculated. The most stable conformer (A) is a symmetrical one with two Me on the side of the hydrogen bond and two hydrogens on the side of the CN (Figure 2A), which is 5.92 kcal/mol more stable than the most stable amide conformer. It is 9.9 kcal/mol more stable than the other symmetrical conformation (B) with two Me groups on the side of the CN (Figure 2B). The two other conformations are (C1) with Me on the amide side and Me on the CN side (Figure 2C), and (C2) Me on the enol side and Me on the CN side which are 3.36 and 3.72 kcal/mol, respectively, less stable than conformer A. An indication for the steric repulsion is given by the dihedral angle between the C−C=C and C−CN planes. This angle is 180° for systems with at least one H near the CN, for example, for conformers A, C1, and C2 and for the unsubstituted cyanomalonamide (R^1-R^4 = H), meaning that the CN and the six-membered enolic ring are in the same plane. In contrast, when two Me groups reside close to the CN as in conformer B or the tetra-Me compound (R^1-R^4 = Me), the dihedral angles are 169 and 163°, respectively. The distances between the CN carbon and the Me hydrogen close to it are 2.747 and 2.746 Å in B, 2.746 Å in C1, 2.751 Å in C2, and 2.747 and 2.510 Å in the tetra-Me compound.

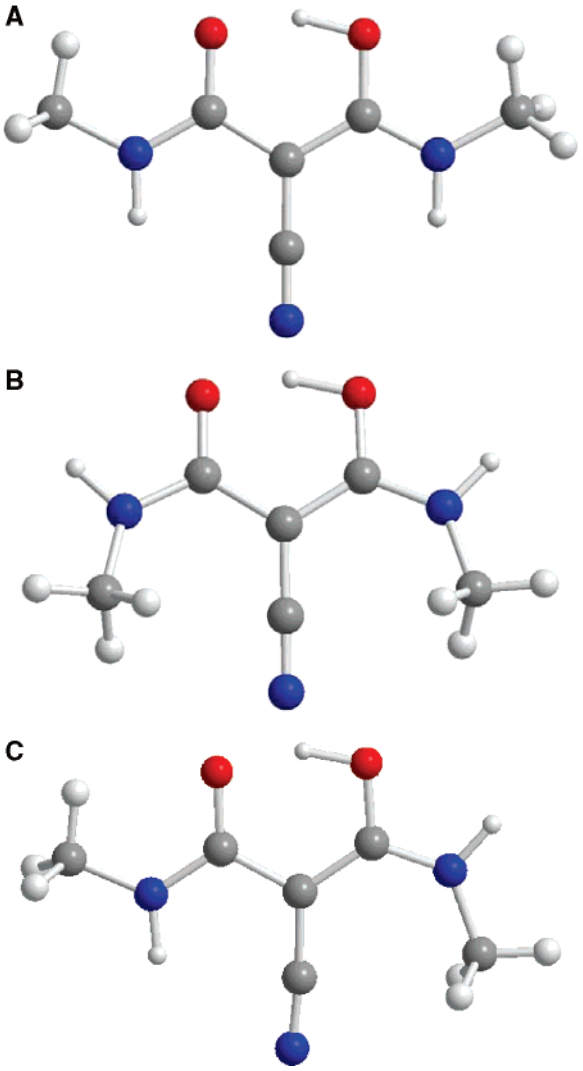

FIGURE 2. Calculated structures (B3LYP/6-31G**) for several conformations of MeNHCOC(CN)=C(OH)NHMe: (A) Me groups close to the O−H···O bond; (B) Me groups close to the CN group; (C) one Me close to the O−H···O bond and one close to the CN.

The energy difference between conformers A and B, which translates to pK_{Enol} of ca. 3 for B, seems inconsistent with the pK_{Enol} of −2.1 for the tetramethyl derivative (Table 2). If only the effect operating for B applies, the observed value obtained

(11) Mishima, M.; Matsuoka, M.; Lei, Y. X.; Rappoport, Z. *J. Org. Chem.* **2004**, *69*, 5947.

is at least 6 kcal/mol too negative. We ascribe this to hydrogen bonding in the corresponding malonamides. The bond for the Me_4 derivative cannot be stabilized by an intramolecular N−H···O═C hydrogen bond, whereas that of B has such stabilization. In summary, the *relatively* small difference of 3.6 pK_{Enol} units between the tetra-H and tetra-Me compared with 7.2 units between conformers A and B is due to a combination of destabilization of the enols by electronic and steric effects of the Me groups and destabilization of the tetramethyldiamide by lack of H-bonding.

These results point to a source of a possible up to 1 kcal/mol difference between the calculated and observed pK_{Enol} values. The calculated values are for the difference between the most stable conformers of the amide and the enol. In solution, there may be rapid equilibria between more than two conformers with the most stable one, which may give a more negative calculated pK_{Enol} value.

These energy differences between conformers and the resemblance of K_{enol} of the **4f/5f/6f** and the **4s/5s/6s** systems with the bulky CPh_3 and $CHPh_2$ substituents to those of enols with smaller substituents suggest that in the conformations of these enols the bulky groups occupy positions remote from the CN group, so that steric effects are less pronounced than they may be for the higher energy conformers. Moreover, the diamides in these cases can form intramolecular hydrogen bonds.

Steric effects clearly affect the preferred conformation and presumably the pK_{Enol} values. In either the observed or the calculated preferred conformation, the two *N*-substituents adjacent to the CN group are the smaller ones, usually two hydrogens.

Isodesmic Reactions. When presenting eq 1, we suggested that the effect of EWGs on K_{Enol} is mainly due to enol stabilization by structure **1b**. However, amide destabilization probably due to repulsion between the lone pairs on the nitrogen and the oxygen carbonyl was found to be considerable in several previously published systems.[1b] We probed this question together with the *N*-substituent effect by isodesmic reactions 5−8, which eliminate the interaction between the "functional" and "substituent" amide or enol groups.

$$R^1R^2NCOCH(CN)CONR^3R^4 + CH_4 \rightleftharpoons CH_3CONR^1R^2 + R^4R^3NCOCH_2CN \quad (5)$$

$$R^1R^2NCOC(CN)═C(OH)NR^3R^4 + CH_4 \rightleftharpoons CH_2═C(OH)NR^1R^2 + R^4R^3NCOCH_2CN \quad (6)$$

$$R^1R^2NCOCH(CN)CONR^3R^4 + H_2C═CH_2 \rightleftharpoons CH_3CONR^1R^2 + R^4R^3NCOC(CN)═CH_2 \quad (7)$$

$$R^1R^2NCOC(CN)═C(OH)NR^3R^4 + H_2C═CH_2 \rightleftharpoons CH_2═C(OH)NR^1R^2 + R^4R^3NCOC(CN)═CH_2 \quad (8)$$

The calculations were conducted by transfer of an amide or an enol group to either CH_4 or $H_2C═CH_2$. The three symmetrical systems R^1, $R^2 = R^3$, R^4 =H, H, H, Me, and Me, Me were used. In the data given in Table 3, positive values indicate that the "reactants" are more stable than the "products" and vice versa. The following conclusions arise from Table 3. (a) The stabilization of the malonamide/its enol pair compared with the acetamide/its enol pair is obtained from eq 9, which is the difference between eqs 5 and 6 or eqs 7 and 8. The values are very high, being 36.8 kcal/mol for the H, H and H, Me systems and 31.9 for the Me, Me systems. This gives the pK_{Enol} values of Table 2 when the literature values for acetamide and *N*,*N*-dimethylacetamide at the B3LYP/6-31G** level of 28.9 and 28.8 kcal/mol[3] are considered. (b) The major effect is indeed

$$R^1R^2NCOCH(CN)CONR^3R^4 + CH_2═C(OH)NR^1R^2 \rightleftharpoons R^1R^2NCOC(CN)═C(OH)NR^3R^4 + CH_3CONR^1R^2 \quad (9)$$

stabilization of the enol, whereas destabilization of the amide amounts to a lower percent of the overall effect. This differs from systems which are activated by two cyano substituents.[1c] (c) The overall effect of the methyl groups is not systematic. Whereas the ΔG_9 value is the smaller of the two Me groups, the values for H, H and H, Me are identical. Clearly, the effect of the two Me groups is smaller, but the effect of one H and one Me group on the enol stabilization is the highest. Speculatively, this may be due to steric effect between the two Me groups and the CN in the planar enol form. The effect on the amide is the smallest for the H, Me system.

TABLE 3. ΔG Values (kcal/mol) for the Isodesmic Reactions 5−8

$R^1R^2 = R^3R^4$	eq	ΔG
H, H	5	-0.7
	6	36.1
	7	-10.4
	8	26.4
H, Me	5	0.8
	6	37.5
	7	-9.0
	8	27.8
Me, Me	5	-2.2
	6	29.7
	7	-9.8
	8	22.1

TABLE 4. Calculated pK_{Enol} Values (B3LYP/6-31G) for Some Activated Amides Y′YCHCONH$_2$**

Y′/Y=	CN	$CONH_2$	CO_2Me	NO_2	NO
H	11.0[a]	5.8[b]	5.3		
CN	-0.2	-5.7	(-5.5)[c]		
CO_2Me	-5.5	-5.8	-4.4		
$CONH_2$	(-5.7)[c]	1.4	(-5.8)[c]	-8.5[d]	-14.2[e]

[a] Exp. 9.22 (H_2O). [b] Exp. 9.1 (H_2O). [c] Appears twice in the table. [d] −6.7 for enol on the NO_2 group. [e] −18.9 for enol on the NO group.

Carboxamide as a Promoting Group for Enol Formation. The high % enol in DMSO and DMF, the lower field δ(OH), and the short H-bond (see below) give the impression that an amido group is a better enol formation promoter than the previously studied ester or even CN groups. Although there is no unequivocal correlation between the σ^- value of a substituent and its ability to promote enolization, we note that the σ_p^- (σ_R^-) values of CO_2R, CN, and $CONH_2$ groups are 0.74, 1.02, and 0.62 (0.31, 0.26, 0.23), respectively,[12] so that in our systems, the weaker negative charge delocalizing substituent by resonance ($CONH_2$) is the better enol formation promoter.

Comparison of some calculated pK_{Enol} values for EWG-substituted amides including malonamides in the gas phase are of interest (Table 4). For enolization of malonamide, methyl malonamate, and cyanoacetamide, pK_{Enol} = 5.8, 5.3, and 11.0,

(12) Charton, M. In *The Chemistry of Organolithium Compounds*; Rappoport, Z., Ed.; Wiley: Chichester, 2004; Vol. 1, Chapter 7, p 267.

respectively. This is due to the feasibility for hydrogen-bond stabilization in the two former compounds which is lacking in the cyanoacetamide. Williams' experimental values in water[13] are higher, being 9.1 (malonamide) and 9.22 (cyanoacetamide).[13b] On replacing one of the hydrogens in YCH_2CONH_2 with a CO_2-Me group, K_{Enol} increases for Y = CN, $CONH_2$, or CO_2Me by 10.8−11.5 orders of magnitude, and the ester-substituted malonamide is slightly more enolic than the other derivatives. In the system $YCH(CN)CONH_2$ for Y = CO_2Me and $CONH_2$, the % enol is nearly the same but is substantially less for Y = CN, probably due to the lack of hydrogen bonding in the enol.

For malonamide itself, pK_{Enol} = 5.8. With an additional carbamido group, the amide is still more stable than the enol (pK_{Enol} = 1.4), due to the nonplanarity of the enol resulting from steric repulsion between two NH_2 moieties. However, when other EWG substituents replace the H, the enol becomes much more stable (Table 4): with CN or CO_2Me groups, pK_{Enol} = −5.7 and −5.8. $O_2NCH(CO_2NH_2)_2$ is more enolic: pK_{Enol}= −8.5 and enolization on the nitro group is calculated to be 1.8 pK_{Enol} units less favorable (pK_{Enol} = −6.7).[10] This trend is reversed for the nitroso-substituted system when the pK_{Enol} values are −14.2 and −18.9 for enolization on the amide and the NO group, respectively. Indeed, NO compounds give the oxime in CH−NO systems and are stable only in the absence of H.[14]

There are few other cyanodiamide systems that can be *experimentally* compared with the analogous cyanoester−amide systems. The effect of a CO_2Me group in $NCCH(CO_2Me)$-$CONHR$ cannot be compared when R = Ph since the signals for the enol and the amide coalesce at rt[1b] and the K_{Enol} value is unavailable. However, comparison is possible when R = *i*-Pr.[1e] From Table 5 for COX, $K_{Enol}(CONH_2) > K_{Enol}(CO_2Me) > K_{Enol}(CONHMe)$ in both $CDCl_3$ and CD_3CN. Comparison of δ(OH) values shows that the OH signal is at a >3 ppm lower field in the diamides than in the ester amides. This applies to the other amide/ester comparisons below. However, δ(OH) in the diester amides is much closer to that in the cyanodiamides. From the K_{Enol} values, $CO_2CH_2CF_3$ is a better enol formation promoter[1c] than the *N*-methylated CONHMe in $CDCl_3$ and in CD_3CN, but the relationship is inverted in one of the two cases studied in THF-d_8. However, a non-*N*-methylated $CONH_2$ group is somewhat more activating than $CO_2CH_2CF_3$, and the effect is larger in THF for R = Ph, An, whereas for R = *i*-Pr the two groups show similar effect in CD_3CN. This is in line with the calculations above. Finally, $K_{Enol}(CO_2CH(CF_3)_2) > K_{Enol}$-(CONHMe),[1c] although we cannot conclude unequivocally that $K_{Enol}(CO_2CH(CF_3)_2) > K_{Enol}(CONH_2)$ since the hexafluoroester derivative ionizes in DMF-d_7.[1b] However, the inequality seems to hold, as judged by indirect comparison of other values in Table 5. We conclude that there is no special effect in malonamides on K_{Enol} values compared with ester-substituted systems, except for the relatively high K_{Enol} values in DMSO and DMF.

Crystallographic Data. We conducted an extensive crystallographic structure determination of many amide/enol systems in order to answer the following questions: (a) What is the structure of the isolated crystals, and is there a correlation between the % enol in a certain solvent (e.g., the pK_{Enol} in $CDCl_3$) and the structure of the isolated solid species, similar to that found previously?[1c] (b) Do the C═C bond lengths in the enols elongate as observed with other enols substituted by EWGs,[1] and if so, to what extent? (c) What is the substituent effect on the preferred enolization site in systems carrying two different CONRR′ groups, and are the two possible regioisomers formed in one system? (d) Is the configuration of the solid enol *E* or *Z*, and is it determined by intramolecular hydrogen bonding as found previously?[1c−f] (e) Can we isolate crystals of both isomeric enol and amide under different conditions. (f) What are the substituent and temperature effects on the nature and symmetry of the hydrogen bond? (g) What is the effect of a possible resonance-assisted hydrogen bond on crystallographic parameters of the enol? (h) Are NHR groups which are not intramolecularly hydrogen bonded, intermolecularly bonded?

TABLE 5. Comparison of "Enol Promoting" Groups in RNHCOCH(CN)COX

R	X	solvent	K_{Enol}	δ(OH)
Ph	OCH_2CF_3	$CDCl_3$	≥50	14.37
		THF-d_8	5	14.42
		CD_3CN	1.44	14.04
Ph	NHMe(H)	$CDCl_3$	9.0 (≥50)	17.65 (17.32)
		THF-d_8	5.25 (32)	18.18 (17.35)
		CD_3CN	1.08 (4.9)	17.98 (17.29)
An	OCH_2CF_3	$CDCl_3$	≥50	14.37
		THF-d_8	10	14.00
		CD_3CN	2.33	14.04
An	NHMe(H)	$CDCl_3$	9	17.71
		THF-d_8	5.7 (13.3)	18.25 (17.54)
		CD_3CN	1.33 (4.3)	17.96 (17.43)
i-Pr[a]	OCH_2CF_3	$CDCl_3$	≥50	14.37
		CD_3CN	5.3	13.98
i-Pr	NHMe(H)	$CDCl_3$	11.5 (≥50)	17.73 (17.53)
		THF-d_8	9.0 (≥50)	18.44 (17.89)
		CD_3CN	11.7 (5.25)	18.11 (18.39)
		DMF-d_7	0.85 (3.55)	18.39 (18.00)
i-Pr[a]	OCH_3	$CDCl_3$	48	14.81
		CD_3CN	1.8	14.93
		DMF-d_7	1.9	14.95
i-Pr[a]	OCH_2CF_3	$CDCl_3$	≥50	14.37
		THF-d_8	≥50[b]	
		DMF-d_7	*c*	

[a] From ref 1e. [b] Probably ionizes completely. [c] Ionizes completely.

Concerning question (h), the enols take advantage of hydrogen-bonding stabilization when possible. Intramolecular hydrogen bonds between OH and O and NRR′ groups are discussed below, but when these cannot be formed, intermolecular H-bonds are formed. The CN group is incapable of forming an intramolecular H-bond in our systems due to its geometry, but a common feature is that the cyano group's nitrogen on one enol molecule is hydrogen bonded to the N−H group of another enol molecule.[1b,d] Figure 3 shows such an intermolecular dimer for **5o**, with a CN···H−N hydrogen bond length of 2.193 Å, an N···N nonbond distance of 3.030 Å, and a N···H−N angle of 158.85°. The O···O nonbonding distance in the intramolecular O−H···O═ hydrogen bond is much shorter, 2.408 Å, and hence much stronger. A similar intermolecular CN···H−N hydrogen bond in enol $MeCO_2C(CN)$═$C(OH)NHPh$[1b] is of approximately the same length (2.07 Å).

We determined 13 structures of amide/enol systems by X-ray crystallography. Although the % enol in $CDCl_3$ is high (≥80%) for all of them, four of them display an amide structure, and nine display an enol structure in the solid (Table 6). In none of

(13) (a) Williams, D. L. H.; Xia, L. *J. Chem. Soc., Chem. Commun.* **1992**, 985; *J. Chem. Soc., Perkin Trans. 2* **1993**, 1429. (b) Eberlin, A.; Williams, D. H. L. *J. Chem. Soc.* **2002**, 1316.

(14) (a) Smith, M. B.; March, J. *March's Advanced Organic Chemistry*, 5th ed.; Wiley: New York, 2001; p 76. (b) The oxime was identified as the nitrosation product of methylmalonic acid: Barry, R. H.; Hartung, W. H. *J. Org. Chem.* **1947**, *12*, 460.

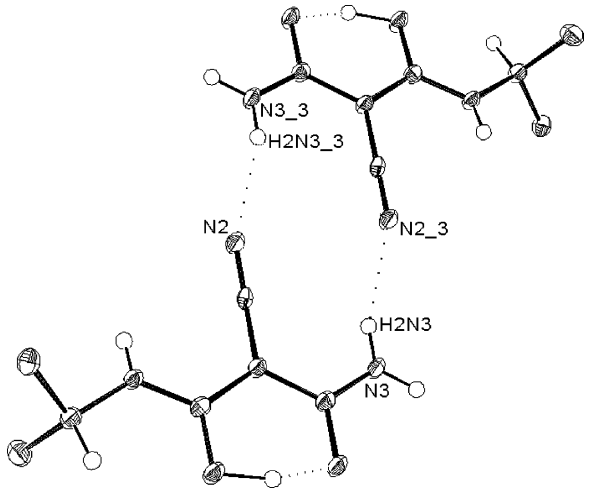

FIGURE 3. The intermolecular CN···H−N bond in the solid structure of enol **5o**. (The term "_3" stands for the (crystallographic) operation $-x, -y, 1-z$ needed to produce the second molecule.)

our systems did we isolate *separate* crystals of the amide and the enol. We had recently isolated separate crystals of the cyanothiomalonamide MeNHCSCH(CN)CONHMe and its enol,[15] a related system to our compounds.

For all systems with an amide structure, $R^1 = Me$, whereas $R^2 = Me$, $R^3 = p$-An, *i*-Pr, or $R^2 = H$, $R^3 = Ph$, *t*-Bu (**4b**, **4d**, **4g**, and **4k** with 80, 80, 90, and 84% enol, respectively, in $CDCl_3$). These values are mostly lower than those for the other species having an enol structure. Consequently, there is no strong correlation between the % enol in solution and the solid-state structure. The solid-state structure is not necessarily that of the main species observed in solution, in contrast with our previous experience with the diester-substituted amides.[1c,f] The X-ray structure of **4k** is given in Figure 4.

The Solid-State Enols. (a) Observed Structures and Temperature Effect. The $CONMe_2$/CONHPr-*i* system is 80% enolic in $CDCl_3$ but gives amide crystal structure at 298 K. In contrast, when the $CONMe_2$/CONHPh analogue (**6a**) is crystallized from $CDCl_3$, EtOAc/petroleum ether mixture, or DMF-d_7/H_2O mixture, it displays at 293 K an enol structure (Figure 5), whose O−H bond is formed on the NMe_2-bound carbonyl. The two O−H(O···H) distances of the hydrogen-bonded enol moiety O−H···O are d_5 = O−H = 1.15 Å, d_6 = H···O = 1.26 Å; that is, the difference Δ_{OH} ($=d_6 - d_5$) of 0.11 Å is not very large. The O···O distance of 2.38 Å is very short, and the O−H···O angle is 158°. The enolic C═C bond is elongated to 1.417 Å, and the C−O bond is a single bond at 1.293 Å. Consequently, the two C−C bonds around the cyano-bound carbon differ by only 0.08 Å, whereas the formal C═O and C−O bonds differ by 0.042 Å.

From the data for **6a** at a lower temperature of 123 K (Figure 5), the main feature is that the OH is still on the same former carbonyl, but the O−H bond is somewhat elongated (Δ_{OH} = 0.34 Å), and the H-bond is much less symmetric. The bond angle of 159.5(19)° is nearly the same as that in 293 K. Interestingly, Δ_{CO} = (d(C−O) − d(C═O) = C(1)O(1)−C(3)O(2) = $d_1 - d_4$) remains nearly the same, whereas the C−C bonds differ by only Δ_{CC} = (d(C═C) − d(C−C) = C(1)C(2)−C(2)C(3) = $d_2 - d_3$) = 0.012 Å. A similar temperature effect is shown also for the CONHMe/ CONHAn-*p* (**5h**) enol.

Table 6 gives selected crystallographic data for the 13 amide/enol structures. The full data are in the crystallographic information files in the Supporting Information. Interesting parameters are the bond lengths for the pairs of C−C, C−O, and O−H bonds, their differences Δ_{CO}, Δ_{CC}, and Δ_{OH}, the nonbonded O···O distance, and the O(1)HO(2) hydrogen bond angle. Also given is the % enol in $CDCl_3$, which is our least polar solvent and hence the one that mostly "resembles" an isolated molecule, and δ(OH) in $CDCl_3$. The calculated (B3LYP/6-31G**) bond lengths and angles for several of the compounds for which experimental data are available are given in Table 6 in bold font.

As expected, in the four amide structures (entries 3, 5, 6, and 10), the Δ_{CC} and Δ_{CO} values are small and within the combined experimental errors. Only enol **5j**/**6j** has a low *R* factor (0.12), and the hydrogen position is of low accuracy, but the enol structure is clear. Seven of these structures were determined at a single temperature, but those of **6a** were determined at 293 and 123 K and of **5h** at 295 and 123 K. The major temperature-dependent difference is in the O−H···O bond. At 123 K, the two O−H bonds were somewhat longer than the quoted "normal" O−H bond of 0.967 Å,[16] being 1.05 Å (**6a**) and 1.02 Å (**5h**). The corresponding O···H lengths d_6 were 1.39 and 1.47 Å, respectively. At the higher temperature, there is an approach to O−H bond equalization for **6a** (Figure 5), whereas for **5h**, the bond lengths are closer than at 123 K but still differ significantly (1.17 and 1.30 Å).

A similar trend of higher differences (higher Δ_{OH}) at the lower temperature is deduced from the collected single temperature Δ_{OH} values for other enols: −0.48 (**6i** at 173 K), −0.50 (**5s** = **6s** at 123 K), −0.13 (**5n** at 123 K), and −0.05 (**6q** at 295 K). This is not always the case: a low value of −0.196 (for **5o** at 100 K) and a relatively high value of −0.45 (for **6c**) at 295 K were also found. We realize that, due to the general difficulty in locating the hydrogen, especially at the higher temperature,[17] the Δ_{OH} parameter is a priori of a lower accuracy than the Δ_{CC} and Δ_{CO} parameters. The observed O−H···O bond angles are 153−164°.

(b) Calculated Structures. The eight calculated structures ("**Cal**" in Table 6) reasonably match the X-ray determined structures, remembering that the calculations are for a single molecule in the gas phase and for a static molecule. A dynamic process leads to averaging of the bond lengths of two isomeric static structures (see below) and is partially responsible for the difference between some of the observed and calculated values. The calculated O−H···O bond angles are 153.0−156.4°, that is, mostly somewhat lower than the X-ray values. Other calculations are discussed below.

If the tendency for bond equalization is due to a rapid hydrogen shift between two regioisomeric enols (see below), it should be reflected in a similar tendency for temperature-dependence bond equalization in the C−C or C−O bonds, that is, to lower Δ_{CC} and Δ_{CO} values at a higher temperature. The problem with this probe is that the difference in the relevant

(15) Basheer, A.; Rappoport, Z. *Org. Lett.* **2006**, *8*, 5931.

(16) Allen, F. H.; Kennard, O.; Watson, D. G.; Brammer, L. E.; Orpen, A. G.; Taylor, R. *J. Chem. Soc., Perkin Trans. 2* **1987**, S1.

(17) (a) Dunitz, J. D. *X-ray Analysis and the Structure of Organic Molecules*; Cornell University Press: Ithaca, NY, 1979. (b) Allen, F. H.; Bellard, S.; Brice, M. D.; Cartwright, B. A.; Doubleday, A.; Higgs, H.; Hummelink, T. W. A.; Hummelink-Peters, B. G. M. C.; Kennard, O.; Motherwell, W. D. S.; Rodgers, J. R.; Watson, D. G. *Acta Crystallogr.* **1979**, *B35*, 2331. (c) Allen, F. H.; Davies, J. E.; Galloy, J. E.; Johnson, J. J.; Kennard, O.; Macrae, C. F.; Mitchell, G. F.; Smith, J. M.; Watson, D. G. J. *Chem. Inf. Comput. Sci.* **1991**, *31*, 187.

TABLE 6. Crystallographic and Calculated (B3LYP/6-31) Data for Substituted Cyanomalonamides/Enols 4/5/6**

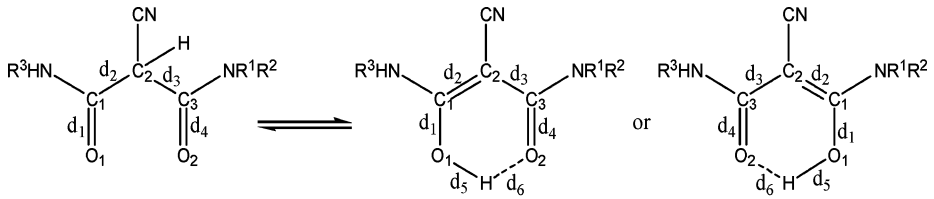

4 **5** **6**

no.	compd	NR^1R^2	R^3	species	% enol, and (OH) in $CDCl_3$[a]	T (K)	C(1)−C(2) (d_2)	C(2)−C(3) (d_3)	Δ_{CC}	C(1)−O(1) (d_1)	C(3)−O(2) (d_4)	Δ_{CO}	O(1)−H (d_5)	O(2)···H (d_6)	Δ_{OH}	Δ (O···O)	<OHO
1	**6a**	NMe_2	Ph	enol	−	123	1.4259(19)	1.4382(19)	-0.0123(38)	1.3020(16)	1.2608(16)	0.0412(32)	1.05(2)	1.39(2)	-0.34(4)	2.4011(14)	159.5(19)
2	**6a**	NMe_2	Ph	enol	80, 17.79	293	1.417(3)	1.435(3)	-0.018(6)	1.293(4)	1.251(2)	0.044 (6)	1.15(4)	1.26(4)	-0.11	2.376(3)	158(3)
2Cal	**6a**	**NMe_2**	**Ph**	**enol**	−	**0**	**1.423**	**1.465**	**-0.042**	**1.315**	**1.262**	**0.053**	**1.048**	**1.428**	**-0.38**	**2.423**	**156.0**
3	**4b. H_2O**	NMe_2	*p*-AnC_6H_4	amide	80	295	1.534(3)	1.549(3)	-0.015(5)	1.218(3)	1.226(3)	0.008(6)	−	−	−	−	−
4	**6c**	NMe_2	C_6F_5	enol	93, 16.82	295	1.420(5)	1.434(5)	-0.014(10)	1.311(4)	1.256(4)	0.055(8)	1.01(4)	1.46(4)	-0.45(8)	2.419(4)	158(4)
5	**4d**	NMe_2	*i*-Pr	amide	80	298	1.545(3)	1.532(4)	0.013(6)	1.232(3)	1.220(3)	0.012(6)	−	-−	-−	-−	-−
5Cal	**4d**	**NMe_2**	***i*-Pr**	**amide**	−	**0**	**1.553**	**1.569**	**-0.016**	**1.227**	**1.216**	**0.011**	−	−	−	−	−
6	**4g**	NHMe	Ph	amide	90	100	1.547(3)	1.543(3)	0.004(6)	1.205(3)	1.224(3)	−0.019(6)	−	−	−	−	−
7	**5h**	NHMe	*p*-AnC_6H_4	enol	90, 17.71	295	1.401(5)	1.440(5)	-0.039(10)	1.301(4)	1.277(4)	0.024(8)	1.17(5)	1.30(5)	-0.13(10)	2.424(4)	159(4)
8	**5h**	NHMe	*p*-AnC_6H_4	enol	−	123	1.414(2)	1.451(2)	-0.037(4)	1.304(2)	1.277(2)	0.027(4)	1.02(3)	1.47(3)	-0.45(6)	2.4409(18)	158(3)
8Cal	**5h**	**NHMe**	***p*-AnC_6H_4**	**enol**	−	**0**	**1.419**	**1.454**	**-0.035**	**1.306**	**1.267**	**0.039**	**1.065**	**1.409**	**-0.344**	**2.423**	**156.4**
9	**6i**	NHMe[c]	C_6F_5	enol	97, 16.70	173	1.409(2)	1.423(2)	−0.014(4)	1.2989(19)	1.2469(19)	0.052(38)	0.95(3)	1.57(3)1.47(3)	-0.62(6)	2.4552(17)	153(2)
							1.410(2)	1.423(2)	−0.013(4)	1.2921(19)	1.2513(19)	0.041(38)	0.99(3)		-0.48(6)	2.4203(16)	159(3)
9Cal	**6i**	**NHMe**	**C_6F_5**	**enol**	−	**0**	**1.419**	**1.446**	**-0.027**	**1.310**	**1.255**	**0.055**	**1.038**	**1.485**	**-0.445**	**2.461**	**154.0**
10	**5j/6j**	NHMe	*i*-Pr	enol	92, 17.73	295	1.443(9)	1.452(9)	-0.009(18)	1.306(8)	1.300(8)	0.006(16)	1.12(14)	1.36(14)	0.24(28)	2.446(7)	163(10)
10Cal	**5j/6j**	**NHMe**	***i*-Pr**	**enol**	−	**0**	**1.416**	**1.454**	**-0.038**	**1.311**	**1.260**	**0.051**	**1.051**	**1.444**	**-0.393**	**2.440**	**155.6**
11	**4k**	NHMe	*t*-Bu	amide	84	295	1.548(4)	1.531(4)	0.017(8)	1.214(3)	1.227(3)	-0.013(6)	−	−	−	−	−
12	**5n**	NH_2	C_6F_5	enol	100, 16.23	123	1.413(2)	1.4312(18)	-0.016(4)	1.2794(19)	1.2911(15)	-0.0114(34)	1.17(3)	1.30(3)	-0.13(6)	2.4148(13)	157(2)
12Cal	**5n**	**NH_2**	**C_6F_5**	**enol**	−	**0**	**1.412**	**1.450**	**-0.038**	**1.310**	**1.253**	**0.057**	**1.033**	**1.505**	**-0.472**	**2.471**	**153.0**
13	**5o**	NH_2	*i*-Pr	enol	100, 17.53	100	1.4234(16)	1.4283(17)	-0.005(33)	1.2935(14)	1.2835(14)	0.010(28)	1.12(3)	1.31(3)	-0.19(6)	2.4085(12)	164(2)
13Cal	**5o**	**NH_2**	***i*-Pr**	**enol**	-	**0**	**1.409**	**1.458**	**-0.049**	**1.309**	**1.265**	**0.044**	**1.050**	**1.452**	**-0.402**	**2.443**	**155.0**
14	**6q**[b]	NHPh	C_6F_5	enol	100, 17.27	295	1.412(6)	1.417(5)	-0.005(11)	1.273(5)	1.270(5)	0.003(10)	1.20(6)	1.25(6)	-0.05(12)	2.414(5)	160(5)
15	**5s=6s**	NHPr-*i*	*i*-Pr	enol	92, 17.76	123	1.425(3)	1.446(3)	-0.021(6)	1.307(3)	1.277(3)	0.030(6)	0.99(3)	1.49(3)	-0.50(6)	2.427(2)	156(3)
15Cal	**5s=6s**	**NHPr-i**	**i-Pr**	**enol**	−	**0**	**1.417**	**1.425**	**-0.008**	**1.311**	**1.268**	**0.043**	**1.055**	**1.436**	**-0.381**	**2.437**	**155.8**

[a] Both parameters were measured at room temperature. [b] Crystallizes with 1.5 molecules of C_6H_6. [c] Two independent molecules in the asymmetric unit. Crystallizes with two molecules of EtOAc.

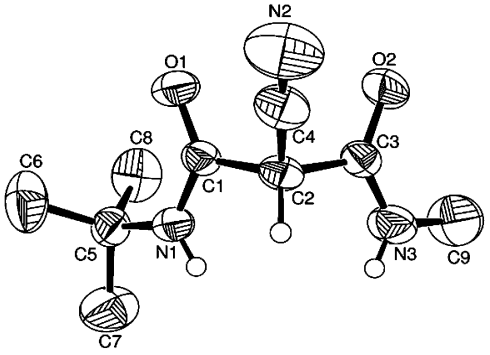

FIGURE 4. ORTEP structure of amide **4k**.

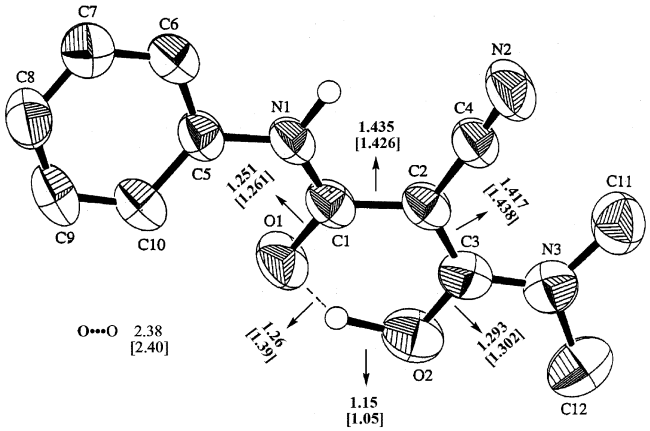

FIGURE 5. ORTEP structure of enol **6a** at 293 K (no brackets) and 123 K [in square brackets].

bond lengths is a priori not large. The C═C bond length is 1.332 Å, and in enones C_β═C_α−C═O, it is 1.340 Å, whereas the central formal single bond length is 1.464 Å.[16] However, our enols are dipolar push−pull alkenes with an important contribution from structure HO(RR'N)C^+-C^-(CN)CONR″R‴, so that $d_2 \gg 1.332$ Å, and in many activated enols similar to **5** and **6**, it is usually 1.41−1.42 Å,[1] and the Δ_{CC} value should be relatively small even at low temperature.[18] The C−O bond in enols is 1.333 Å, and a C═O bond in the enones is 1.222 Å.[16] However, in the dipolar structure, the C═O double bond is elongated due to some single bond character, and Δ_{CO} is expected to decrease. Indeed, even at the low temperature, the Δ_{CC} and Δ_{CO} terms are relatively small. Only in four of the enols is the Δ_{CC} value higher than the combined experimental error in d_2 and d_3, and in three remaining cases, it is <0.01 Å. Only for **5h**, Δ_{CC} of 0.03 Å at 123 K becomes 0.01 Å at 295 K. Note that the two bond lengths of **6a** are identical within their combined errors at 123 K but are somewhat different at 298 K. Consequently, the Δ_{CC} probe alone is of little help in studying the dynamic process.

A similar analysis of the C═O and C−O bonds is more encouraging. In contrast with the Δ_{CC} values of −0.05 to −0.021 Å for all systems, except of −0.039/−0.037 for **5h**, the Δ_{CO} values are larger, being 0.003−0.055 Å, indicating a potentially higher change with the temperature. For **6a**, the two C−O bonds differ significantly, but the Δ_{CO} is almost temperature-independent. For **5h**, Δ_{CO} is somewhat higher at the lower

(18) Note that the hydrogen bond strongly reduces the polarity of the enols, as shown by the solvent effect on pK_{Enol} values.

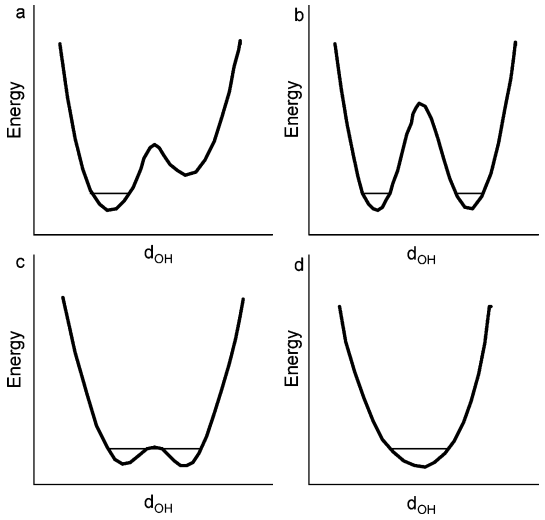

FIGURE 6. Different PESs for the hydrogen bond.

temperature, but at 295 K, it is at the limit of the combined experimental errors. For **6c** at 295 K, the difference is significant as shown by the Δ_{OH} values. For **5j/6j**, **5n**, and **6q** at 295 K, the Δ_{CO} values are close to zero considering their errors, whereas for **5s** = **6s** at 123K and for **6i** at 173 K, Δ_{CO} is significant, and for **5o** at 100 K, the lengths differ slightly.

Gilli suggested that the coordinate of the antisymmetric vibration of the enolone moiety $Q = d_1 - d_2 + d_3 - d_4 = \Delta_{CO} - \Delta_{CC}$ is a better measure than the individual Δ_{CC} and Δ_{CO} terms and tabulated a variety of Q values for many enol systems.[20a,c,g] Remarkably low Q values of 0.013, 0.015, 0.005, and 0.008 were found for **5j**/**6j**, **5n**, **5o**, and **6q**, respectively, whereas the eight other values for seven enols were 0.061 ± 0.006. The calculated seven values are higher, being 0.083 ± 0.012.

A major concern in the solid-state structure is the nature of the hydrogen bond. The two amido groups are structurally mostly similar and sometimes identical, raising the question of symmetry of the bond. The nature of the hydrogen bond is usually discussed in terms of the four potential energy surfaces (PES) shown in Figure 6.[19] When the energies of the two possible hydrogen-bond arrangements formed by a proton shift between the oxygens differ significantly, the PES is an asymmetric double-well potential (Figure 6a). If the energies are similar, the symmetric double-well potential PES (Figure 6b) is obtained. A decrease of the proton-transfer barrier leads to the low barrier hydrogen bond PES (Figure 6c), and if the barrier is very small or disappears, a single-well potential PES (Figure 6d) is obtained. The stronger the hydrogen bond, the lower the barrier. The hydrogen bond strength is related to the nonbonded O···O distance, and distances of <2.5 Å are ascribed to strong hydrogen bonds.[19] In our enols, the values are 2.38−2.46 Å (Table 6), the bonds are strong hydrogen bonds, and the barriers for hydrogen transfer are presumably low.

(19) Perrin, C. L.; Nielson, J. B. *Annu. Rev. Phys. Chem.* **1997**, *48*, 511.
(20) (a) Gilli, G.; Belluci, V.; Ferretti, V.; Bertolasi, V. *J. Am. Chem. Soc.* **1989**, *111*, 1023. (b) Gilli, G.; Bertolasi, V. In *The Chemistry of Enols*; Rappoport, Z., Ed.; Wiley: Chichester, 1990; Chapter 13, p 713. (c) Bertolasi, V.; Gilli, P.; Ferretti, V.; Gilli, G. *J. Am. Chem. Soc.* **1991**, *113*, 4917. (d) Bertolasi, V.; Gilli, P.; Ferretti, V.; Gilli, G. *J. Chem. Soc., Perkin Trans. 2* **1997**, 945. (e) Gilli, P.; Bertolasi, V.; Ferretti, V.; Gilli, G. *J. Am. Chem. Soc.* **2000**, *122*, 10495. (f) Bertolasi, V.; Gilli, P.; Ferretti, V.; Gilli, G. *New J. Chem.* **2001**, *25*, 408. (g) Gilli, P.; Bertolasi, V.; Pretto, L.; Ferretti, V.; Gilli, G. *J. Am. Chem. Soc.* **2004**, *126*, 3845.

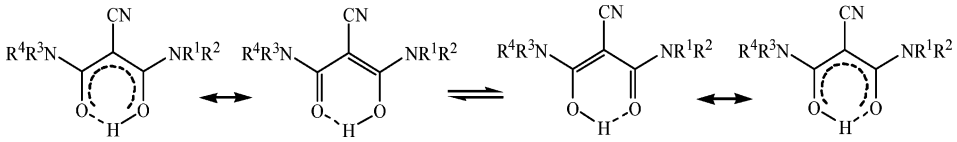

FIGURE 7. Resonance-assisted hydrogen bond of two equilibrating structures.

Following Gilli's analysis for the structurally related enols of 1,3-diketones,[20] and the temperature effect on the bond lengths, the enol is depicted as two structures in rapid equilibrium, each of which is stabilized by resonance, that is, being a resonance-assisted hydrogen-bonded structure (Figure 7).[20]

As shown in Figure 7, both enols have a *Z* configuration, regardless whether hydrogen migration takes place. If it occurs, together with the known rapid rotation around the formal single $C_\alpha-C_\beta$ bond character in the zwitterionic enol,[1c] four enols can be potentially observed, that is, *E*,*Z* pairs of each of the two regioisomeric enols on the two amido carbonyls. The observation of only a single enol, in contrast with the observation of *E*,*Z* pairs for enols RNHC(OH)═C(CO_2R')CO_2R,[1c,f] indicates much less stable *E* structures. This is not surprising since the only intramolecular hydrogen bonds possible in them are O···H−N and N···H−N bonds, which are weaker than the O···H−O bond.[6]

The temperature effect on Δ_{OH}, Δ_{CC}, and Δ_{CO} values (Table 6) may suggest an apparent more symmetric structure at the higher temperature. This is ascribed to a rapid proton shift between the regioisomeric enol structures (Figure 7). At a low temperature, this process is relatively slow, and mainly one static structure of the double minimum surface is observed. At a higher temperature, the hydrogen transfer rate approaches the measurement time scale and we see higher "formal" symmetry at 293 and 295 K due to partial or complete averaging of the bond lengths of the two equilibrating structures (cf. Figure 6c). The error in the X-ray determination of the hydrogen position calls for a corroboration of this suggestion, which is obtained from the DFT calculations (Table 6), which show in all cases at 0 K a nonsymmetrical structure, even for **5s** = **6s**, which is a chemically symmetrical system.

The calculated O−H bond lengths for **6a** and **5h** are somewhat longer than the normal value for an O−H bond, and the O−H and O···H bond lengths are much closer to the experimental values at 123 K than at 293 K; for **6i**, they fit the values at 173 K considering the experimental error and for **5n** the calculated Δ_{OH}(cal) > Δ_{OH}(exp) even at 100 K. Due to this error, the comparison between the calculated and experimental C−C and C═C bond lengths is less satisfactory, although the calculated C═C bond is longer (or identical for **5n**) than the experimental value, whereas the trend for the C−C bond is less clear. Consistently, Δ_{CO}(cal) > Δ_{CO}(exp). The conclusion from all these data supports the assumption of a nonsymmetrical hydrogen bond with a slow hydrogen movement between two regioisomeric enols at the low temperature and a faster shift at the higher temperature. We assume a faster hydrogen shift in solution, and since our measurements were at room temperature, a fast mutual isomerization of enols **5** and **6** takes place in solution.

O···O and δ(OH) Values. A short O···O distance in the solid and a low-field δ(OH) in solution are regarded as probes of strong hydrogen bonds.[20] A correlation between the two parameters is close to linear, and distances of 2.38−2.46 Å are associated with δ(OH) values of >16 ppm.[20c] All of our compounds show the two parameters in this region (Table 6), but good correlation between them was not observed. The four compounds with δ(OH) = 17.7−17.8 display O···O distances of 2. 38−2.46 Å, and the lowest δ(OH) = 16.23 corresponds to O···O of 2.415 Å. This can be understood since the three lower δ(OH) values in Table 6 are when $R^3 = C_6F_5$, an EWG. Both the electron withdrawal and the ring current may affect the δ(OH) and probably do not affect the O···O in a similar way.

The Enolization Site. The enolization site in the crystals of solid enols is deduced from X-ray crystallography. Due to our assumption of the rapid proton shift, there is little meaning to the "site of enolization" at rt for several systems. No general rule for all X-ray determined structures can be deduced from Table 6, but the calculated energy difference between the two "regioisomeric" enols is low. Remembering these limitations, three of our five systems bearing an aryl group on one nitrogen and a single alkyl or two alkyls on the other nitrogen enolize on the alkyl-substituted amido group, and two carrying an electron-withdrawing *p*-anisyl group (**5h**) and an electron-donating C_6F_5 group (**5n**) enolize near the aryl site. When an *i*-PrNH group competes with H_2N or MeNH group, enolization is near the *i*-PrNH.

The energy differences between regioisomeric enols of cyanomalonamides were calculated for seven cases (Table S4) and account for the lack of a generalization for the enolization site. The differences are very small, being 0.01−0.7 kcal/mol for **5j**, **5m**, **6c**, **6d**, **6n**, and **6o** over **6j**, **6m**, **5c**, **5d**, **5n**, and **5o**, respectively. Hence, in half of the cases, there is ca. 1:1 ratio of both isomers, and in the other cases, there is at least 23% of the minor isomer. The barriers for the regioisomer interconversion are presumably low, based on the temperature effect in the solid enols and the O···O values, and hence both species exist in appreciable amounts in solution. Since the amide is sometimes formed when the enol is ≥80% of the mixture in solution, and with an energy difference of <0.6 kcal/mol between the two isomers, either of them can be crystallized, depending on differences in crystal packing. Consequently, it is not surprising that the calculations of Table S4 match two X-ray determined isomers, do not match it in other two cases, and the amide is formed in another case.

IR Spectra (a) of the Solid Species. The solid-state structures of systems for which we lack X-ray crystallographic data were analyzed by IR spectra of the solid species in KBr or in nujol. The absorptions were very similar in both media. The regions of interest are those of the CN and the OH. The 2100−2300 cm^{-1} region is that applied for detecting CN stretch, although usually, the common range studied is 2260−2200 cm^{-1}, with stronger absorption toward its lower end for conjugated cyano groups.[21] In cyano carbanions, the wavenumbers are lower than those of conjugated nitriles.[21b] Our 20 solid systems studied show two types of behavior. Five show mainly or exclusively a signal in the narrow range of 2252−2257 cm^{-1}, and **4k** displayed absorption at 2264 cm^{-1}. These are saturated CN group stretchings and compounds **4b**, **4d**, **4g**, and **4k** whose

TABLE 7. IR Absorptions for $R^3NHCOCH(CN)CONR^1R^2$ (KBr,[a] cm^{-1})

R^3	R^1	R^2	compd	ν_{CN}	ν_{CO}	ν_{NH}	ν_{OH}	ν_{other}
				Group A[b]				
t-Bu	H	H	**4p**	2255.5	1715, 1684	3392, 3310, 3076	2560	2751
t-Bu	H	Me[c]	**4k**	2264	1697, 1653	3328, 3126, 3061	2660	
Ph	H	Me[c]	**4g**	2254	1702, 1663	3323, 3281, 3209,3147, 3110, 3056		1966
t-Bu	Me	Me	**4e**	2253.5	~1700, 1682	3761, 3287, 3078	2600	
i-Pr	Me	Me[c,d]	**4d**	2252	~1670	3299, 3077	2550, 2655	
p-An	Me	Me[c]	**4b**	2257	1663	3486, 3417, 3313, 3256	2680	1899, 2046, 2530
				Group B[f]				
i-Pr	H	H	**5o**	2200, 2148[g]	1643	3416, 3336, 3243	2698	2474, 1811
C_6F_5	H	H	**5n**	2200, 2149[g]	1637	3437, 3342, 3309	2699	1765, 2464
p-An	H	H	**5/6m**	2202	1648	3422, 3319, 3248	2550, 2675	
Ph	H	H	**5l**	2201, 2180[g]	1648	3420, 3324, 3048	2680	1788
i-Pr	H	Me	**5j**	2195, 2166[g]	-	3340, 3313	2685	1917, 2475
C_6F_5	H	Me	**6i**	2213, 2161[g]	1633	3324, 3214, 3025	2670	2468
p-An	H	Me[e]	**4h**	2197, 2253	1673	3392, 3322, 3287, 3208, 3136, 3069	2600	1887
C_6F_5	H	Ph	**5q**	2207,2195[h]	1645	3411, 3251	2674	ca. 1900
$CHPh_2$	H	$CHPh_2$	**5t**	2198,2254[g]	1682	3289		1880,1900
i-Pr	H	*i*-Pr	**5/6s**	2189, 2137[g]	1640	3338	2685	1945,2435
Ph	H	Ph	**5/6r**	2196, 2137[g]	1650	3489, 3406, 3257, 3057[g]		
Ph	Me	Me	**5g**	2196,2144[g]	1651	3293, 3195, 3065	2630	1800,1906,2470
C_6F_5	Me	Me	**5i**	2204,2192[h]	1651	3241	2660	1901,2454

[a] Also in nujol. [b] Amide according to IR. [c] Amide according to X-rays. [d] With D_2O: new signals at 2415, 2450 cm^{-1}. [e] Enol according to X-rays. [f] Enol or mostly enol according to IR. [g] Weak. [h] Medium.

X-ray diffraction was determined, belong to Group A of Table 7. The correspondence between X-ray structure and IR data of the solid enables the determination, with some confidence, of the solid-state structure of a species whose X-ray data are unavailable.

All of the three solid amides with one *t*-BuNHCO group and a second H_2NCO, MeNHCO, or Me_2NCO group (100, 84, and 73% enol in $CDCl_3$, respectively) belong to this group. They also display CO signals at 1697−1715 and 1653−1684 cm^{-1}. The other three compounds display signals at 1663−1702 cm^{-1}, the approximate ranges of solid primary and secondary amide absorptions.[21a]

All Group A compounds display 3−6 absorptions in the 3486−3056 cm^{-1} range, which are assigned to the several amido NH groups. Table 7 give the CN, NH, and C═O absorptions in KBr.

When D_2O is added to solid **4d**, new signals appear at 2415 and 2450 cm^{-1}, which are ascribed to the labeled CONDPr-*i* and OD groups.

Most of the compounds (Group B, Table 7) display a strong signal at 2189−2207 cm^{-1} (mostly at the narrow range of 2195−2200 cm^{-1}) and at 2213 cm^{-1} in one case. These are in the range and even lower than that ascribed to unsaturated nitriles, such as the enols. Each of them displays an additional weak signal at 2136−2185 cm^{-1} which may be relevant to the intermolecular N−H/CN H-bonds in the solid. They also display signals which may be the amide I N−H bending signal at 1633−1651 cm^{-1}.[21a] Several signals appear at >3047 cm^{-1} which we ascribe to NH stretchings, but even in the enols, there is still one amido group which absorbs >3050 cm^{-1}. The weak absorption in the range of 2560−2699 cm^{-1} is ascribed to the strong O−H···O bonds, based on the weak[22a] ν_{OH} of 2500[22b] or 2566−2675 cm^{-1} for enols of 1,3-diketones.[20c] Additional small signals which appear in the 1800 and 1900 cm^{-1} ranges for most compounds were not identified.

TABLE 8. IR Absorptions (cm^{-1}) of Selected Formal $R^1R^2NHCOCH(CN)CONHR^3$ in $CHCl_3$ Solution

R^3	R^1	R^2	compd	ν_{CN}	ν_{CO}	ν_{NH}
p-An	H	H	**5/6m**	2194	1670	3430, 3392
C_6F_5	H	H	**5/6n**	2206	1648	3420 (br), 3356, 3302
t-Bu	H	H	**5/6p**	2192	1698 (w)	3524, 3483, 3416 (br)
i-Pr	H	*i*-Pr	**4/5/6o**	2187, 2259 (w)	1697	3420, 3327
C_6F_5	H	Me	**5/6i**	2197	1644	3435, 3331
t-Bu	H	Me	**4/5/6t**	2169, 2253	1716	3420, 3347
Ph	Me	Me	**4/5/6a**	2188, 2255	1654, 1700	3409, 3299
C_6F_5	Me	Me	**5/6c**	2194	1648, 1717	3403, 3252
t-Bu	Me	Me	**4/5/6e**	2183, 2254	1655	3419, 3307

Solid compounds **4h** and **5t**, which display CN signals in both the saturated and the unsaturated regions, apparently contain significant percentages of both the amide and enol.

IR Spectra (b) in $CHCl_3$ Solution. In $CHCl_3$, the $CONH_2$-substituted systems and some other derivatives have very low solubility, resulting in low-intensity signals. Almost all compounds display conjugated CN signals at 2169−2206 cm^{-1}. A weak signal for a saturated CN does not appear in the $CONH_2$ derivatives, but a medium or weak signal at 2252 ± 3 cm^{-1} is observed in most other derivatives. CO signals at 1655−1715 cm^{-1} are observed when the saturated CN signal is significant. There are signals >3050 cm^{-1} for all compounds, but an extensive band at 3200−2500 cm^{-1}, including the O−H···O peak (see above), was not observed, except for a weak signal at 2669 cm^{-1} for **5i**. Consequently, the spectra are not informative in relation to the hydrogen bonding.

Table 8 gives CN, CO, and NH absorptions in $CHCl_3$ for selected enols/amides, and Table S5 in the Supporting Information gives additional IR data. Enol signals are observed in all

(21) (a) Silverstein, R. M.; Bassler, G. C.; Morrill, T. C. *Spectrometric Identification of Organic Compounds*, 4th ed.; Wiley: Chichester, 1981; pp 129−130. (b) Juchnovski, I. N.; Binev, I. G. In *The Chemistry of Functional Groups, Supplement C: The Chemistry of Triple-bonded Functional Groups*; Patai, S., Rappoport, Z., Eds.; Wiley: Chichester, 1983; Chapter 4, p 107.

(22) (a) Kopteva, T. S.; Shigorin, D. N. *Russ. J. Phys. Chem. (Engl. Transl.)* **1974**, *48*, 532. (b) Vener, M. V. In *Hydrogen-Transfer Reactions*; Hynes, J. T., Klinman, J. P., Limbach, H.-H., Schowen, R. L., Eds.; Wiley-VCH: Weinheim, Germany; Vol. 1, p 273.

solutions, and additional amide signals are observed in several of them, as judged by similar CN absorptions which are similar to those in the solid state. Comparison with the data in Table 1 shows that only unsaturated CN absorptions appear for completely enolic systems in $CHCl_3$, whereas saturated CN absorptions appear for systems which display both enol and amide in solution.

Conclusions. All of the *N*-substituted cyanomalonamides studied form the *Z*-enols in solution. A rare feature is the presence of an appreciable % enol in DMF-d_7 and DMSO-d_6. The temperature-dependent bond length changes in the X-ray structure suggest a dynamic proton transfer between regioisomeric enols in the solid state. The short O···O nonbonded distances indicate a strong hydrogen bond, and calculations indicate it to be nonsymmetrical. Substituent and solvent effects were determined. The isolated crystals are not necessarily those of the more abundant species in solution.

Experimental Section

General Methods. Melting points, ^{1}H and ^{13}C NMR and IR spectra were measured as described previously.[23] All of the commercial precursors and solvents were purchased from Aldrich.

***N*-Methylcyanoacetamide.** To methyl cyanoacetate (19.8 g, 0.2 mol) at −10 °C was added a solution of 40% aqueous methylamine (25 mL, 0.29 mol) dropwise with stirring, while retaining the temperature below 0 °C. A white solid was obtained, and the mixture was stirred for an additional 1 h at 0 °C and for 3 h at room temperature. Most of the solvent was evaporated, the remaining solid was filtered and dissolved in ethyl acetate (200 mL), the solution was dried (Na_2SO_4), and the solvent was evaporated, giving 15.7 g (0.16 mol, 80%) of *N*-methylcyanoacetamide, mp 108 °C (lit.[24] 101 °C): ^{1}H NMR (DMSO, rt) δ 2.60 (3H, d, J = 4.6 Hz, Me), 3.58 (2H, s, CH_2), 8.14 (1H, br s, NH).

***N*-Isopropylcyanoacetamide.** To methyl cyanoacetate (9.9 g, 0.1 mol) at 0 °C was added isopropylamine (8.5 mL, 0.1 mol) dropwise at <10 °C. After stirring for 1 h, water (10 mL) and NaOH (0.1 g) were added and the white solid *N*-isopropylcyanoacetamide obtained (4.8 g, 0.04 mol, 40%), mp 82 °C (lit.[24] 65 °C; lit.[25] 73−74 °C), was filtered: ^{1}H NMR ($CDCl_3$, rt) δ 1.19 (6H, d, J = 6.6 Hz, Me), 3.35 (2H, s, CH_2), 4.06 (1H, octet, J = 7.0 Hz, CH), 6.10 (1H, br s, NH); ^{13}C NMR ($CDCl_3$, rt) δ 22.28 (q, J = 126.8 Hz, Me), 25.91 (t, J = 136.9 Hz, CH_2), 42.62 (d, J = 140.4 Hz, CH), 114.84 (s, CN), 159.98 (s, C═O).

Cyanoacetanilide was prepared similarly from methyl cyanoacetate and aniline, mp 196−8 °C (lit.[26] 198 °C; lit.[27] 203−205 °C): ^{1}H NMR ($CDCl_3$, 298 K) δ 3.50 (2H, s, CH_2), 7.20 (1H, t, J = 7.3 Hz, Ph−H), 7.37 (2H, t, J = 8.0 Hz, Ph−H), 7.51 (2H, d, J = 8.1 Hz, Ph−H), 7.67 (1H, br s, NH).

***N*-Diphenylmethylcyanoacetamide,**[28] mp 123−5 °C, was prepared similarly from methyl cyanoacetate and diphenylmethyl amine: ^{1}H NMR ($CDCl_3$, 298 K) δ 3.89 (2H, s, CH_2), 6.21 (1H, d, J= 7.9 Hz, CH), 6.73 (1H, d, J = 7.0 Hz, NH), 7.22−7.38 (10H, m, 2Ph).

***N,N*-Dimethylcyanoacetamide.** A 40% aqueous solution of Me_2H (40 mL, 0.35 mol) was added to methyl cyanoacetate (19.8 g, 0.2 mol) at −10 °C. The mixture was stirred for 1 h at <0 °C and overnight at rt. No precipitate was formed, even after addition of NaOH (0.4 g) and additional stirring for 48 h. The mixture was extracted with AcOEt (2 × 100 mL), the organic phase was dried (Na_2SO_4), and the solvent was evaporated, leaving an oil which gave a crystalline compound after standing overnight. After washing with ether, 14.2 g (0.125 mol, 63%) of *N,N*-dimethylcyanoacetamide, mp 68 °C (lit.[29] 62 °C; lit.[30] 58 °C), was formed: ^{1}H NMR ($CDCl_3$, 298 K) δ 2.94 (3H, s, Me), 3.01 (3H, s, Me), 3.50 (2H, s, CH_2).

Reaction of *N,N*-Dimethylcyanoacetamide with Phenyl, *p*-Anisyl, Pentafluorophenyl, Isopropyl, and *tert*-Butyl Isocyanates. The procedure described for phenyl isocyanate was also applied for the other four isocyanates: To a stirred suspension of Na (0.25 g, 11 mmol) in dry THF (50 mL) was added *N,N*-dimethylcyanoacetamide (1.12 g, 10 mmol). After 4 h, all the Na reacted, hydrogen evolution was ceased, and the sodium salt of the amide precipitated as a white solid. Phenyl isocyanate (1.08 mL, 10 mmol) was added, the solid was dissolved, and the solution turned orange-yellow. The mixture was refluxed overnight, and the solvent was evaporated, leaving the sodium enolate. It was dissolved in DMF (10 mL), and the solution was added dropwise with stirring and cooling to a cold 2 N HCl solution (100 mL). The white oily solid formed was extracted with ethyl acetate (2 × 100 mL). The organic layer was dried (Na_2SO_4), most of the solvent was evaporated, and to the remaining 10 mL was added petroleum ether (5 mL), and the solution was kept overnight in the refrigerator. The white solid obtained was filtered and dried, giving 1.28 g (5.54 mol, 55%) of the enol/amide mixture **4a**/**5a**/**6a**, mp 125−126 °C. Anal. Calcd for $C_{12}H_{19}N_3O_2$: C, 62.34; H, 5.63; N, 18.18. Found: C, 61.97; H, 5.94; N, 18.11.

Suitable crystals of **6a** for X-ray diffraction were obtained by dissolving the crude solid in ethyl acetate, adding petroleum ether, and keeping the solution in the refrigerator for 1 week: ^{1}H NMR ($CDCl_3$ 298 K) displayed signals for 4:1 enol/amide mixture δ (enol) δ 3.23 (6H, s, 2Me), 7.13 (1H, t, J = 7.3 Hz, *p*-H), 7.33 (2H, t, J = 8.3 Hz, *m*-H), 7.43 (2H, d, J = 7.9 Hz, *o*-H), 7.67 (1H, br s, NH), 17.79 (1H, s, OH); δ (amide) 3.02 (s, Me), 3.18 (s, Me), 4.80 (s, CH), 7.13 (t, *p*-H, overlaps), 7.33 (t, *m*-H, overlaps), 7.53 (d, J = 7.9 Hz, *o*-H), 9.16 (br s, NH); ^{13}C NMR ($CDCl_3$, 298 K) δ (enol) 38.33 (q, J = 140.0 Hz, Me), 55.60 (s, C_β), 120.25 (s, CN), 121.19 (d, J = 162.3 Hz), 124.77 (dt, J_d = 163.0 Hz, J_t = 6.8 Hz), 128.89 (dd, J_1 = 161.5 Hz, J_2 = 8.0 Hz), 136.59 (t, J = 8.8 Hz), 171.09 (m), 172.06 (d, J = 3.0 Hz); δ (amide) 36.71 (q, J = 143.2 Hz, Me), 38.15 (q, J = 137.7 Hz, Me), 44.08 (d, J = 138.9 Hz, CH), 113.40 (d, J = 11.3 Hz, CN), 120.25 (d, J = 163.8 Hz), 125.27 (dt, J_d = 162.3 Hz, J_t = 7.5 Hz), 128.93 (dd, J_1 = 161.5 Hz, J_2 = 8.0 Hz), 136.61 (overlaps, 157.63 (d, J = 8.3 Hz), 161.34 (s).

The 4-methoxyphenyl derivative (**4b**/**5b**/**6b**), mp 104 °C, was prepared similarly in 52% (1.37 g) yield. The pentafluorophenyl derivative (**4c**/**5c**/**6c**) was obtained similarly in dry ether as the solvent. The precipitate was obtained after the acidification without extraction by EtOAc. The product, mp 128−129 °C, was obtained in 49% (0.78 g) yield. The *i*-Pr (**4d**/**5d**/**6d**) and *t*-Bu (**4e**/**5e**/**6e**) derivatives, mp 114−115 and 142−143 °C, respectively, were prepared similarly in 20 and 25% yield, respectively, except that acidification gave no solid, which was obtained only after extraction with EtOAc and evaporation of the solvent. Crystals of the *i*-Pr derivative for X-ray diffraction were obtained by cooling its solution in EtOAc/petroleum ether. The triphenylmethyl derivative (**4f**/**5f**/**6f**), mp 157−159 °C, was prepared similarly in 74% yield. The spectral and analytical data are given in Tables 1, S2, S3, and S6.

Reaction of *N*-Methylcyanoacetamide with Phenyl, *p*-Anisyl, Pentafluorophenyl, Isopropyl, and *tert*-Butyl Isocyanates. The

(23) Frey, J.; Rappoport, Z. *J. Am. Chem. Soc*. **1996**, *118*, 3994 and 5169.

(24) Shukla, J. S.; Bhatia, P. *J. Indian Chem. Soc.* **1978**, *55*, 281.

(25) Cossey, A. L.; Harris, R. L. N.; Huppatz, J. L.; Phillips, J. N. *Aust. J. Chem*. **1976**, *29*, 1039.

(26) Gorobets, N. Y.; Yousefi, B. H.; Behrooz, H.; Belaj, F.; Kappe, C. O. *Tetrahedron* **2004**, *60*, 8633.

(27) Diago-Meseguer, J.; Palomo-Coll, A. L.; Fernandez-Lizarbe, J. R.; Zugaza-Bilbao, A. *Synthesis* **1980**, 547.

(28) Lafton, L. BE Patent, 866163 19781020; *Chem. Abstr*. **1979**, *90*, 103986p.

(29) Ben Cheikh, A.; Chuche, J.; Manisse, N.; Pommelet, J. C.; Netsch, K. P.; Lorencak, P.; Wentrup, C. *J. Org. Chem.* **1991**, *56*, 970.

(30) Tkachenko, V. V.; Tregub, N. G.; Knyazev, A. P.; Mezheritskii, V. V. *Rostov. Gos. Zh. Org. Khim.* **1990**, *26*, 638; *Chem. Abstr*. **1990**, *113*, 152224.

reaction is demonstrated for isopropyl isocyanate. To Na (0.25 g, 11 mmol) in dry THF (60 mL) was added *N*-methylcyanoacetamide (0.98 g, 10 mmol) with stirring, and the mixture was refluxed for 24 h, until all the Na was consumed. An orange salt was obtained. A solution of isopropyl isocyanate (1 mL, 10 mmol) in dry THF (20 mL) was added dropwise to the mixture. The solid was mostly dissolved, and the solution was stirred under reflux for 8 h. Removal of the solvent left a brown solid which was dissolved in DMF (10 mL), and the orange solution was added dropwise to a cold 2 N HCl solution (100 mL). The liquid mixture was extracted with ethyl acetate (3 × 100 mL) and washed with water (3 × 100 mL), the organic phase was dried (Na_2SO_4), and the solvent was evaporated, giving 1.18 g (6.45 mmol, 65%) of the solid yellow product (**4j**/**5j**/**6j**), mp 133−134 °C. Anal. Calcd for $C_8H_{13}N_3O_2$: C, 52.46; H, 7.10; N, 22.95; Found: C, 52.74; H, 7.02; N, 23.13.

The *t*-Bu analogue (**4k**/**5k**/**6k**), mp 138 °C, was obtained similarly in 67% yield and crystallized from EtOAc. In the analogous reaction with the aryl isocyanates, the solid was obtained in the acidification stage without extraction by EtOAc. It was washed with water (300 mL).

The product from phenyl isocyanate (**4g**/**5g**/**6g**), mp 140 °C, was obtained in 59% yield. Crystals for X-ray diffraction were obtained after standing for a long time in a 1:20 DMF/H_2O mixture. The 4-methoxyphenyl derivative (**4h**/**5h**/**6h**), mp 148 °C, was obtained in 64% yield, and crystals for X-ray diffraction were obtained from $CDCl_3$. The pentafluorophenyl derivative (**4i**/**5i**/**6i**), mp 170 °C, was obtained in 51% yield. Crystals for X-ray diffraction were obtained by slow evaporation of the EtOAc solvent at rt. The spectral and analytical data for all derivatives are given in Tables 1, S2, S3, and S6.

Reaction of Cyanoacetamide with Phenyl, *p*-Anisyl, Pentafluorophenyl, Isopropyl, and *tert*-Butyl Isocyanates. Except for small differences, the procedure is similar to that described above for the reaction of *N*-methylcyanoacetamide. Longer reaction times of 48−72 h were required for obtaining the sodium salt. The color of the mixtures is mustard yellow. The mixtures were refluxed overnight.

The *N*-phenyl derivative (**4l**/**5l**/**6l**), mp 176−177 °C, the *N*-*p*-anisyl derivative (**4m**/**5m**/**6m**), mp 172 °C, and the *N*-pentafluorophenyl derivative (**4n**/**5n**/**6n**), mp 168 °C, were obtained in 28, 62, and 66% yield, respectively, and crystallized from EtOAc. The *N*-*i*-Pr derivative (**4o**/**5o**/**6o**), mp 166 °C, was obtained in 39% and crystallized from EtOAc/petroleum ether. The *N*-*t*-Bu derivative (**4p**/**5p**/**6p**), mp 162 °C, was obtained in 26% yield. Spectral and analytical data for all compounds are given in Tables 1, S2, S3, and S6.

Reaction of *N*-Isopropylcyanoacetamide with Isopropyl Isocyanate. To a suspension of Na (250 mg, 11 mmol) in dry THF (50 mL) was added *N*-isopropylcyanoacetamide (1.26 g, 10 mmol), and the mixture was stirred overnight at rt until the Na disappeared. To the yellow solid formed was added a solution of isopropyl isocyanate (1 mL, 10 mmol) in dry THF (20 mL) during 20 min, after which the solid was dissolved giving an orange solution. It was refluxed overnight, and the solvent was evaporated, giving the sodium enolate salt: ^{1}H NMR (DMSO-d_6, 298 K) δ 1.00 (12H, d, J = 6.5 Hz, Me), 3.80 (2H, octet, J = 6.6 Hz, CH-*i*-Pr), 4.97 (1H, br s, NH), 8.77 (1H, br s, NH).

The salt was dissolved in DMF (10 mL), and the solution was added dropwise to a cold 2 N HCl solution (100 mL). The white oily solid obtained was solidified after stirring for 5 min, filtered, and washed with cold water (200 mL), giving the product (**4s**/**5s**/**6s**) (1.08 g, 5.1 mmol, 51%), mp 178 °C. Crystals for X-ray diffraction were obtained by slow evaporation of a $CDCl_3$ solution of the compound. Anal. Calcd for $C_{10}H_{17}N_3O_2$: C, 56.87; H, 8.06; N, 19.90. Found: C, 56.42; H, 8.01; N, 19.40. ^{1}H NMR ($CDCl_3$, rt) δ (91% enol) 1.19 (12H, d, J = 6.5 Hz, Me), 4.08 (2H, octet, J = 6.7 Hz, CH-*i*-Pr), 5.29 (2H, d, J = 5.0 Hz, NH), 17.77 (1H, s, OH); δ (9% amide) 1.19 (overlap), 4.08 (overlap), 4.31 (s, CH), 6.77 (s, NH).

A similar procedure was applied for preparing **4r**/**5r**/**6r**, from *N*′-phenylcyanoacetanilide and phenyl isocyanate, **4t**/**5t**/**6t** from *N*-diphenylmethyl cyanoacetamide and diphenylmethyl isocyanate, and **4q**/**5q**/**6q** from *N*-phenylcyanoacetanilide and pentafluorophenyl isocyanate. The spectral and analytical data for these compounds are given in Tables 1, S2, S3, and S6.

An analogous reaction of *N*-*tert*-butylcyanoacetamide gave the solid Na salt in the first step which did not react with *tert*-butyl isocyanate.

Computation Methods. The compounds investigated were optimized by using the Gaussian 98 program[31] at the hybrid density functional B3LYP/6-31G** method,[32] which was extensively used in recent calculations of enols of carboxylic acid derivatives and shown to give pK_{Enol} values reliable within 2 pK_{Enol} units.[3,33] All optimized structures including higher energy conformers were verified by means of their Hessian matrices to be local minima on the potential energy surfaces. K_{Enol} values were calculated from the free energy differences between the amide and enol forms at 298.15 K.

Acknowledgment. We are indebted to the Israel Science Foundation for support, and to Dr. Shmuel Cohen from the Department of Inorganic and Analytical Chemistry, The Hebrew University, for the X-ray structure determination.

Supporting Information Available: Table S1 with relative integration of signals, Tables S2 and S3 with ^{1}H and ^{13}C NMR data for all compounds, Table S4 with calculated energies of the regioisomeric enols, Table S5 with IR spectral data, and Table S6 with microanalyses and mp of all new compounds. The full crystallographic data for the compounds in Table 6 are available as cifs. The material is available free of charge via the Internet at http://pubs.acs.org.

JO070877H

(31) Frisch, M. J.; Trucks, G. W.; Schlegel, H. B.; Scuseria, G. E.; Robb, M. A.; Cheeseman, J. R.; Zakrzewski, V. G.; Montgomery, J. A, Jr.; Stratmann, R. E.; Burant, J. C.; Dapprich, S.; Millam, J. M.; Daniels, A. D.; Kudin, K. N.; Strain, M. C.; Farkas, O.; Tomasi, J.; Barone, V.; Cossi, M.; Cammi, R.; Mennucci, B.; Pomelli, C.; Adamo, C.; Clifford, S.; Ochterski, J.; Petersson, G. A.; Ayala, P. Y.; Cui, Q.; Morokuma, K.; Malick, D. K.; Rabuck, A. D.; Raghavachari, K.; Foresman, J. B.; Cioslowski, J.; Ortiz, J. V.; Stefanov, B. B.; Liu, G.; Liashenko, A.; Piskorz, P.; Komaromi, I.; Gomperts, R.; Martin, R. L.; Fox, D. J.; Keith, T.; Al-Laham, M. A.; Peng, C. Y.; Nanayakkara, A.; Challacombe, M.; Gill, P. M. W.; Johnson, B.; Chen, W.; Wong, M. W.; Andres, J. L.; Gonzalez, C.; Head-Gordon, M.; Replogle, E. S.; Pople, J. A. *Gaussian 98*, revision A.6; Gaussian, Inc.: Pittsburgh, PA, 1998.

(32) (a) Becke, A. D. *Phys. Rev.* **1988**, *A38*, 3098. (b) Lee, C.; Yang, W.; Parr, R. G. *Phys. Rev.* **1988**, *B37*, 785.

(33) (a) Apeloig, Y.; Arad, D.; Rappoport, Z. *J. Am. Chem. Soc*. **1990**, *112*, 9131. (b) Sklenak, S.; Apeloig, Y.; Rappoport, Z. *J. Chem. Soc., Perkin Trans. 2* **2000**, 2269. (c) Yamataka, H.; Rappoport, Z. *J. Am. Chem. Soc.* **2000**, *122*, 9818. (d) Rappoport, Z.; Lei, Y. X.; Yamataka, H. *Helv. Chem. Acta* **2001**, *84*, 1401.